

Radiation Therapy Patient Dose Measurements

TG-120: Overview

IMRT Measurement Tools

- The overall aim of the TG-120 report was to describe the uses and pitfalls of the most relevant IMRT dosimetry systems
- TG-120 highlighted the unique influence of IMRT on their use for each system and provided recommendations for proper operations of specific dosimeters
- This report (*and my presentation*) includes examples of commercial products and should not be considered an endorsement

Dosimetry tools and techniques for IMRT

Daniel A. Low^a
Washington University, St. Louis, Missouri 63110
Jean M. Moran^b
University of Michigan, Ann Arbor, Michigan 48109
James F. Dempsey^c
Varian Incorporated, Cleveland, Ohio 44106

Jeff Dong^a
MD Anderson Cancer Center, Houston, Texas 77010

Mark Oldham^b
Duke University Medical Center, Durham, North Carolina 27710

(Received 23 January 2010; revised 4 October 2010; accepted for publication 4 October 2010;

Published 16 February 2011)

Intensity modulated radiation therapy (IMRT) poses a number of challenges for properly measuring commissioning data and quality assurance (QA) radiation dose distributions. This report provides a review of the dosimetry tools available for IMRT and describes how these tools can be used to support the commissioning and quality assurance requirements of an IMRT program. The proper application of each dosimeter is described along with the limitations of each. The report also highlights the potential use of these dosimeters in conjunction with other dosimeters to support their proper use, along with potential application of 3D dosimetry. Regardless of the IMRT technique utilized, some situations require the use of multiple detectors for the acquisition of accurate dose distributions. This report also describes the use of multiple dosimeters that aide the physicist in the proper selection and use of the dosimetry tools available for IMRT QA and to provide a rationale for proper use of these tools in the measurement of dose distributions for the purpose of IMRT commissioning and measurement-based characterization or verification of IMRT treatment plans. This report is not intended to provide a comprehensive review of commissioning and QA methods for IMRT. Instead, it is intended to provide a detailed description of the dosimeters and the practical aspects of measurements that are unique to IMRT. The methodology of IMRT concerns the application of measurement instruments and their suitability, calibration, and quality control of these instruments. The dosimeters described in this report are not necessarily recommended when incorporating them into a commissioning process or a comprehensive QA program. For example, some dosimeters are not suitable for use in IMRT due to their physical characteristics. These often exhibit limitations with respect to spatial resolution or energy response and need to themselves be commissioned against more established dosimeters. A chain of dosimeters, from source to detector, is often required to obtain the most accurate dose distribution for the patient. This report is intended to describe the characteristics of the components of these systemic dosimeters, phantoms, and dose evaluation algorithms. This work is the report of AAPM Task Group 120. © 2011 American Association of Physicists in Medicine. [DOI: 10.1118/1.354120]

Key words: radiation therapy, dosimetry, intensity modulated radiation therapy, quality assurance, metrology, radiotherapy

TABLE OF CONTENTS

I. DIFFERENCES IN DOSIMETRY REQUIREMENTS BETWEEN CONVENTIONAL RADIATION THERAPY AND IMRT	1314	II.A. Point dosimeters.....	1315
I.A. Dose distribution complexity.....	1314	II.A.1. Ionization chambers.....	1315
I.B. Temporal nature of IMRT dose delivery.....	1314	II.A.2. Semiconductor detectors.....	1317
I.B.1. Photon dose delivery.....	1314	II.A.3. Electrometer and cable performance.....	1318
I.B.2. Electron dose delivery.....	1314	II.A.4. Applications to IMRT.....	1319
I.C. Monitor units.....	1315	III. CONSIDERATIONS FOR THE USE OF POINT DOSEMETERS	1320
I.D. Summary.....	1315	III.A. Two-dimensional dosimetry.....	1321
II. DOSEMETERS.....	1315	III.B.1. Film.....	1321
		III.B.2. Lead foil and array detectors.....	1324
		III.B.3. Computed radiography.....	1325
		III.B. PHANTOMS.....	1325
		III.A. Phantoms types.....	1325

Point Detectors

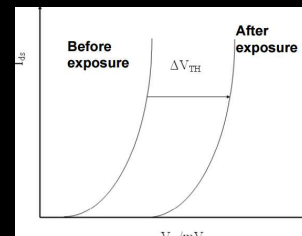
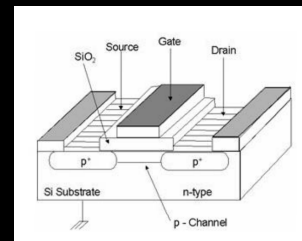
- In radiation therapy, there are many applications for small self-contained dosimeters.
- One of the most common applications for these dosimeters is in-vivo dosimetry.
- There are currently a variety of dosimeters on the market.
 - *Thermoluminescent dosimeters (TLDs)*
 - *Metal oxide semiconductor field effect transistors (MOSFETs)*
 - *Silicon diodes*.
- Each of these detectors has advantages and disadvantages.



MOSFET

Metal Oxide Semiconductor Field Effect Transistor

- Capable of dose measurements immediately after irradiation or can be sampled in predefined time intervals (on-line dosimetry)
- ΔV_T is a function of absorbed dose
- This function is linear when the MOSFET operates in the biased mode during irradiation
- Absorbed dose linearity region increases with the increase of the bias voltage



Soubra, Cygler, Mackay, Med. Phys. 21(4), 567-572, 1994

MOSFET

TN MOSFET type	Bias	Nominal sensitivity (mV/cGy)
Standard sensitivity	Standard	1
Standard sensitivity	High	3
High sensitivity	Standard	3
High sensitivity	High	9

MOSFET

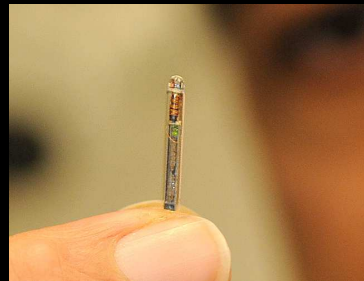
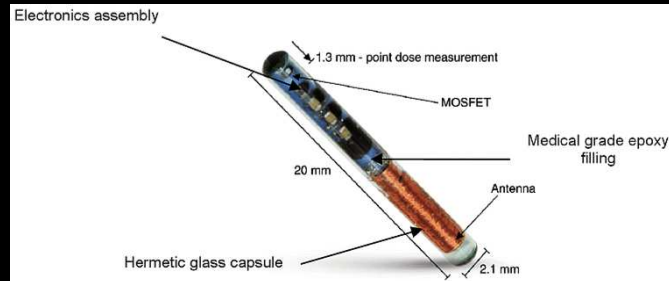
Advantages

- Excellent spatial resolution – small size (~0.04mm)
- Multiple detectors can be irradiated simultaneously
- Automatic and immediate readout
- Can be re-used immediately
- Linear dose response > 30 cGy
- Response independent of depth
- Commercially available phantoms to accommodate the small detectors

Disadvantages

- Decrease linearity for < 30 cGy – limited to high dose applications
- Over-response for the phantom scatter factor for small fields
- Specific application and measurement conditions should be carefully assessed and the detector should be used in the appropriate dose range to maintain response

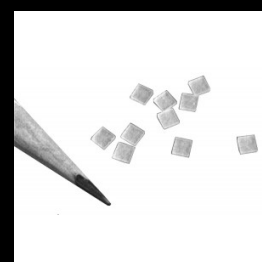
Point Detectors - Implantable



Thermoluminescent Dosimeters

Advantages

- Multiple measurement points in a single irradiation
- Reusable
- Easy to use in multiple phantoms
- Small size and versatility in placement
- Readily available readout equipment
- Achievable accuracy: 2-3%



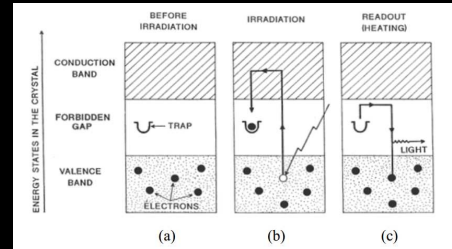
Disadvantages

- Requires calibration to determine calibration factor for each TLD chip
- Requires calibration of subset of TLD chips for each measurement
- TLD reader response and oven temperature should be monitored to maintain response



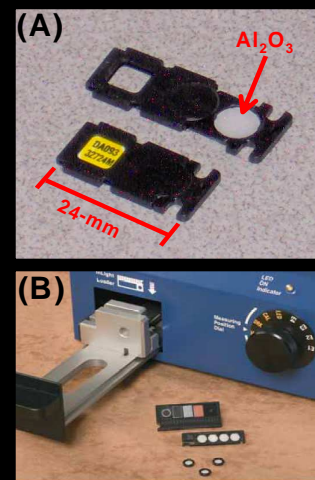
Optically Stimulated Luminescence (OSL)

- OSL is a radiation measurement technique that measures the optically stimulated luminescence of aluminum oxide crystals.
- When irradiated the valence band of the crystals create electron hole pairs.
- If the energy is great enough the electron will move from the valence band to the conduction band.
- In the conduction band the electron loses energy quickly and either falls back to the valence band or becomes trapped.
- Trapped electron will be released when stimulation provides enough energy.



Optically Stimulated Luminescence (OSL)

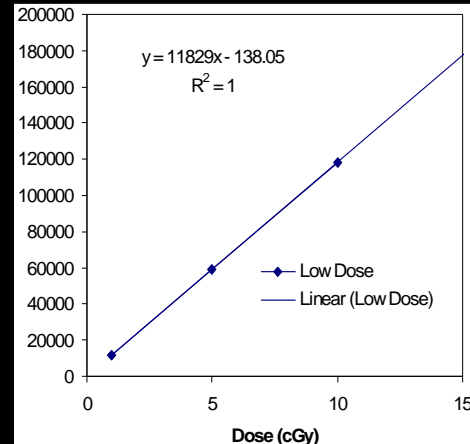
- In the MicroStar system radiation is measured by stimulating the Al_2O_3 material using a green light emitting diode (*LED*).
- Blue light is then emitted from the Al_2O_3 and is directed into a photomultiplier tube (*PMT*).
- The measured luminescence from the detector can be related to the dose using calibrations supplied by Landauer, or created by the user.



OSL Calibration

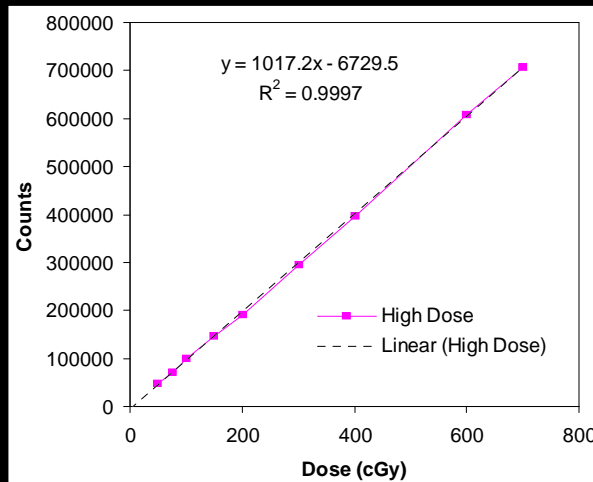
- The system is calibrated by exposing individual dosimeters to known doses between 0 and 700 cGy.
 - 10x10 Field Size
 - 100 SSD
 - 6 MV photons
- MicroStar creates and stores two calibration curves to be used for all future readings.
 - Low Dose (0-10 cGy)
 - High Dose (>10 cGy)

Low Dose Calibration



OSL Calibration

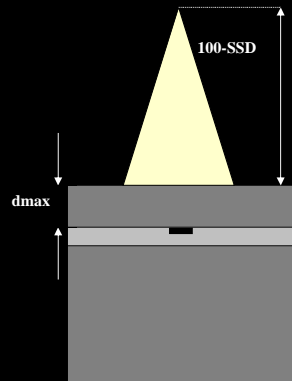
High Dose Calibration



OSL Signal Decay

Signal Decay Setup

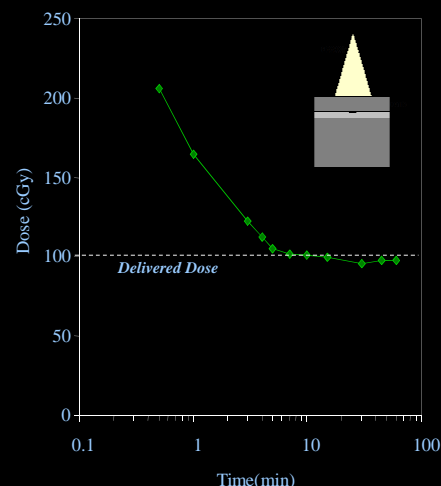
- Due to the ability to read the dosimeters quickly, a signal decay study was completed to find the optimal read time.
 - 100 cGy
 - 10x10 Field Size
 - 100 SSD at d_{max}
 - 6MV photons
 - Varian 21 EX
 - 0.5 - 60 minute intervals



OSL Signal Decay

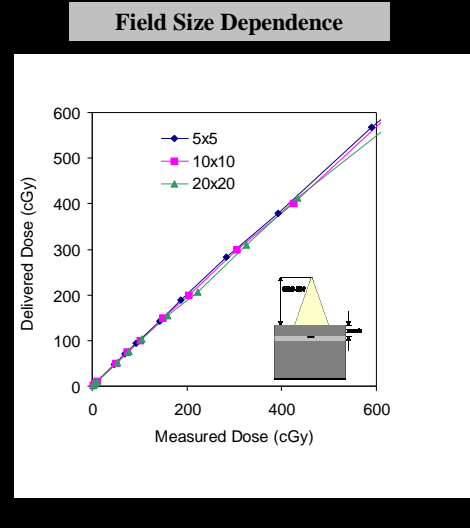
Signal Decay

- There is a significant time dependence within the first 15 minutes after irradiation.
- However, after 10 minutes readings appear within 1%
- Within 2 weeks the dosimeters were continuously monitored and were found to be within 1.1%



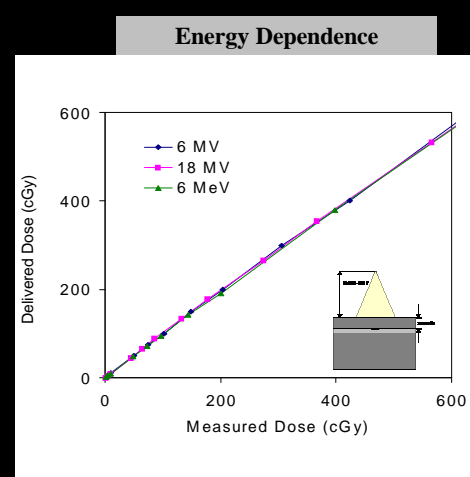
OSL Field Size Dependence

- Readings were taken for 5x5, 10x10 and 20x 20 field sizes on the 21EX using 6MV photons.
- Each chip was placed at 1.5cm depth at 100 SSD with 10cm of backscatter.



OSL Energy Dependence

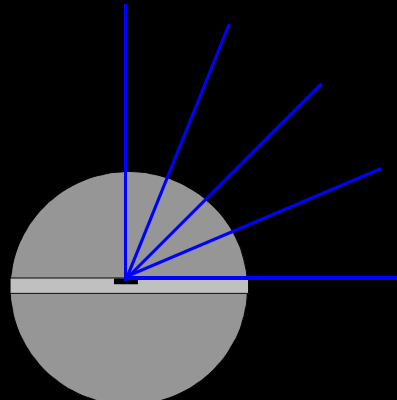
- Readings were taken using 6MV, 18MV and 6MeV beams on the 21EX.
 - 100SSD at dmax
 - 10x10 field size
 - 1-700 cGy
- Unlike silicon diode based dosimetry there isn't an observable field size or energy dependence.



OSL Angular Dependence

- The dosimeters were also evaluated for an angular dependence
- The dosimeters were placed face up in a cylindrical phantom positioned at the isocenter
- 100 MU was then delivered at angles between 0 and 90 degrees.
- The readings were then repeated with the dosimeter placed face down.

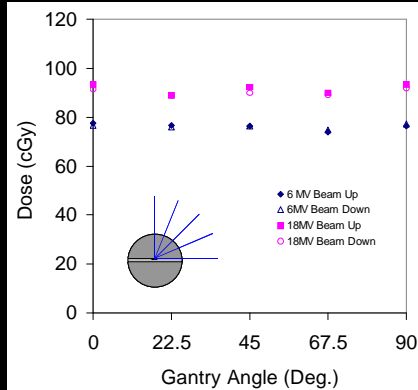
Angular Dependence Setup



OSL Angular Dependence

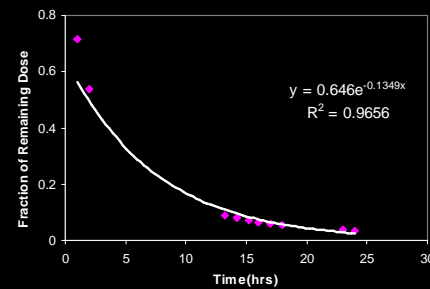
- The variation in response with gantry angle ranged from +1.7 to -2.8% for the 6-MV beam, and +2.0 to -2.8% for the 18-MV beam.
- The variation in response for the beam passing through the back of the detector was 0.1 to 1.4%.
- The results for angular dependence were within the variation in detector response.

Angular Dependence



OSL Dosimeter Blanking

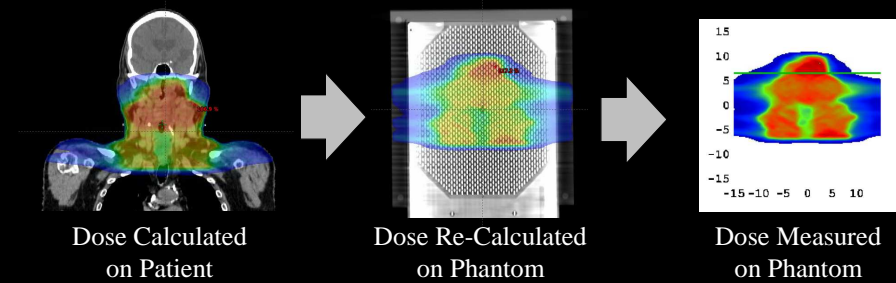
- The ability to erase and reuse the dosimeters was tested by opening the light-proof case and exposing the Al_2O_3 material to ambient room light
- Measurements were taken to determine a decay scheme.
- From the analysis it was found that the half life of the OSL material under normal room light was 5.14 ± 0.01 hours.



Patient Specific IMRT QA

Patient Specific IMRT QA

- Each IMRT patient must have quality assurance performed on their treatment plan
 - *The patient's actual treatment plan is copied to a test phantom*
 - *The radiation is recalculated on the test phantom*
 - *The test phantom is irradiated using the patient's plan*
 - *The calculated and measured doses for the phantom are compared*



Patient Specific IMRT QA

- Each IMRT patient must have quality assurance performed on their treatment plan
 - *Patient Specific IMRT QA can be a time consuming process*
 - *Must be performed by the medical physicist prior to patient treatments*
 - *Rarely finds error according the AAPM Task Group 275 (Plan and Chart Review)*
- Why so we perform patient specific IMRT QA
 1. *To detect errors that can result in patient harm*
 2. *Billing regulations require that it is performed*

Patient Specific IMRT QA

- Scott Jerome-Parks was a computer and systems analyst that worked in lower Manhattan
- In the aftermath of the September 11th attacks, he rushed to the World Trade Center site to help
- In 2004, he began suffering from a nagging sinus infection
- In early 2005, Scott was diagnosed with a Base-of-Tongue primary



Patient Specific IMRT QA

- This photo shows Mr. Jerome-Parks with his wife, Carmen, on the day he received his diagnosis of Base of Tongue cancer
- For his treatment, he chose St. Vincent's Hospital in Manhattan, which was a Varian Medical Systems "Show Site"
- St. Vincent's had been heavily promoting a new Varian linear accelerator and treatment with "Smart-Beam Technology" as a way to solidify its shaky financial standing



Patient Specific IMRT QA

- On a brisk day in March 2005, Mr. Jerome-Parks prepared for his fifth radiation session at St. Vincent's
- His initial treatment plan had IMRT Quality Measurements performed by a medical physicist to verify that the dose was being delivered as prescribed
- After four fractions, Mr. Jerome-Parks Radiation Oncologist asked that the IMRT plan be redone to give more protection to the teeth
- On the morning of March 14, the Eclipse IMRT plan was modified while Mr. Jerome-Parks was waiting in the wings



Patient Specific IMRT QA

- Shortly after 11 a.m., as the Eclipse plan was being saved, the computer began seizing up and displayed an error message
- The hospital would later say that similar system crashes "are not uncommon with the Varian software, and these issues have been communicated to Varian on numerous occasions"
- The error message asked "Do you want to save her changes before the program aborts"
- The treatment planner answered yes, and at 12:24 p.m., the Radiation Oncologist approved the new plan



Patient Specific IMRT QA

- Meanwhile, two therapists began prepping Mr. Jerome-Parks for his procedure on the linac treatment table
- At 12:51 p.m., there was another Varis computer crash at the linac operator console
- By 12:57 p.m., the two therapists had recovered from the crash and began delivering fraction 5 with the new IMRT plan
- The next day, fraction 6 was delivered with the new IMRT plan
- That afternoon a friend told Mr. Jerome-Parks wife “My goodness, look at him. His head and his whole neck were swollen.”



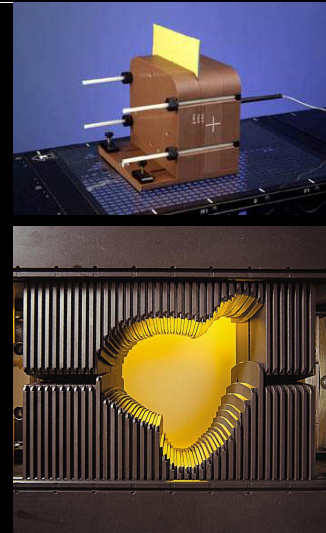
Patient Specific IMRT QA

- Another friend commented “I was shocked because his head was just so blown up. He was in the bed, and he was writhing from side to side and moaning. I just stood at the foot of the bed in the dark and prayed.”
- Ms. Jerome-Parks called the hospital and insisted that someone check if anything was done wrong in the treatment of her husband
- According to the hospital, they sent a psychiatrist to speak to Ms. Jerome-Parks the next day
- A couple of hours later, her husband received fraction 6 with the new IMRT plan



Patient Specific IMRT QA

- At 6:29 p.m. on March 16 (several hours after Mr. Jerome-Parks received his third treatment) the physicist finally performed the IMRT QA for the new plan
- During the plan transfer between Eclipse and VARiS, the MLC shapes did not transfer and all fields were treated with MLC in the parked position
- By 8:15 p.m., the physicist ran the IMRT QA test three times and found the same result
- Mr. Jerome-Parks' entire neck, from the base of his skull to his larynx, had been exposed with the full sliding-window monitor units without any beam shaping



Patient Specific IMRT QA

- During a hospital stay, Mr. Jerome-Parks expressed a wish that he could simply fly away from his troubles
- He had hoped others might learn from his misfortune
- Unfortunately, the details of his case were initially shielded from public view by Varian Medical Systems, the doctors, and the hospital



Patient Specific IMRT QA

Radiation Oncologist

- Starting a patient on an inadequate plan in the first place
- Asking for a rapid re-plan of a complicated technique at short notice

Dosimetrist

- Agreeing to provide a rapid re-plan on a complicated technique

Physicist

- Failure to perform IMRT QA on the new plan

Radiation Therapist

- Not investigating why the switch to open fields on an IMRT Head and Neck Patient
- Why the Monitor Units were so high for open fields

**Where did
it all go
wrong?**



Patient Specific IMRT QA

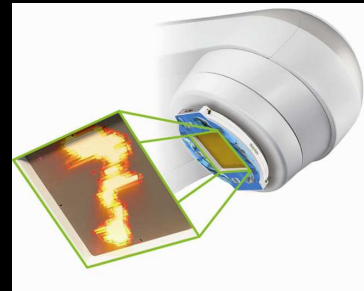
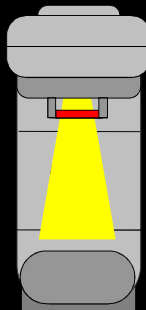
Vendor

- Supplying software capable of saving a partial plan
- An Varian application specialist from the stated off the record that the cause arose because the MLC settings were the last parameters to be saved by the software
- The computer crash left the isodoses and DVHs intact but did not include the MLC settings, which is why the fields were open

**Where did
it all go
wrong?**

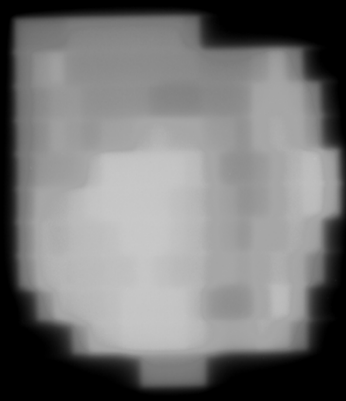
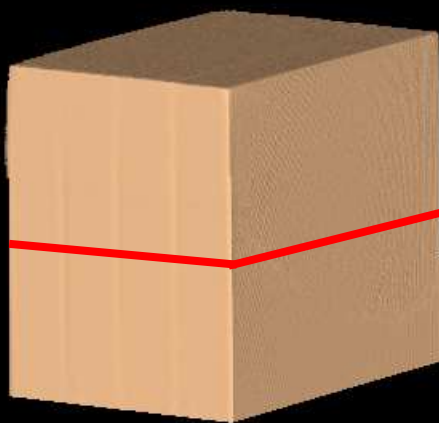


Fluence Maps



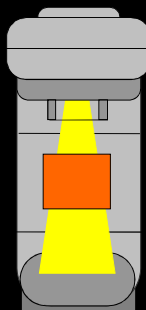
Fluence maps are taken in-air without any build-up

Planar Dosimetry



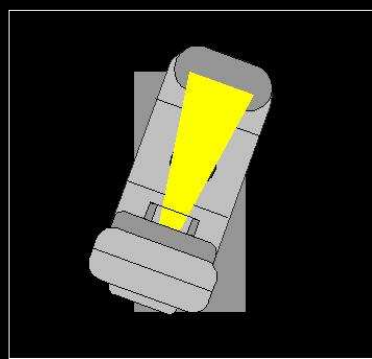
Planar Dosimetry is when measurements are taken with
build-up material one field at a time

Planar Dosimetry



Planar Dosimetry is when measurements are taken with build-up material of one field at a time

Planar Composite Dosimetry

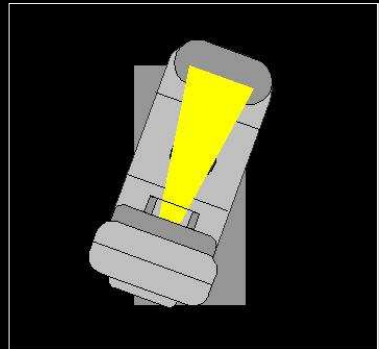


Detector Mounted into Accessory Tray



Planar Composite Dosimetry are measurements taken for all fields from the treatment gantry angles with the detector rotating with the gantry

Planar Composite Dosimetry

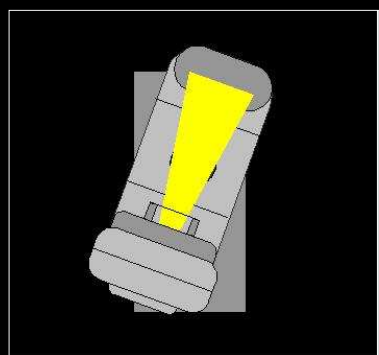


EPID Imager used to Obtain
Measured Dose



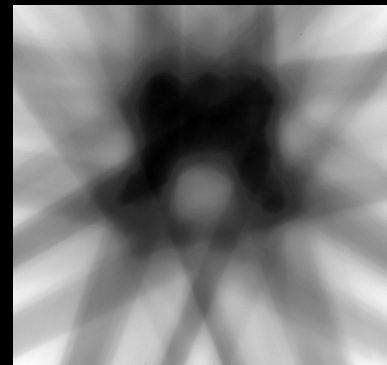
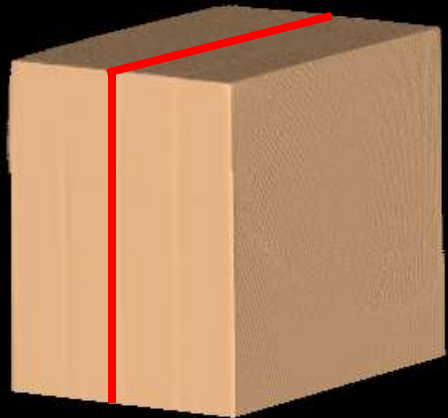
Planar Composite Dosimetry are measurements taken for all fields from the treatment gantry angles with the detector rotating with the gantry

Composite Dosimetry



Composite Dosimetry is when measurements are taken with build-up material for all fields from the treatment gantry angles

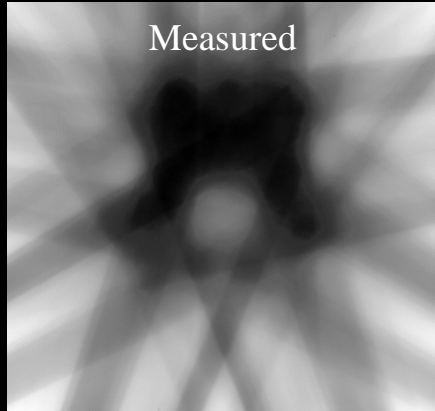
Composite Dosimetry



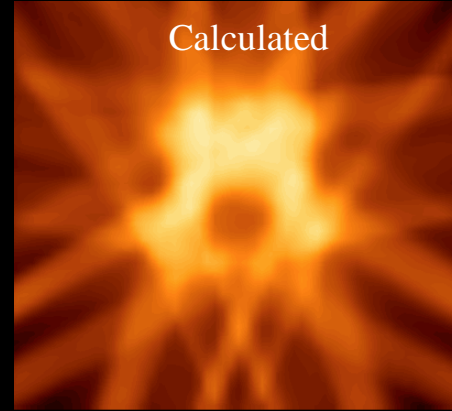
Composite Dosimetry is when measurements are taken with build-up material for all fields from the treatment gantry angles

Composite Dosimetry

Measured

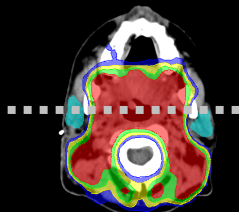
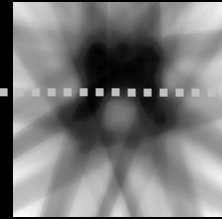
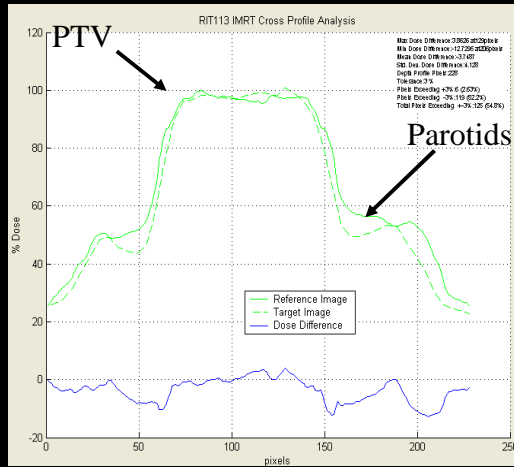


Calculated



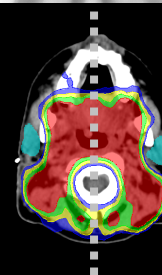
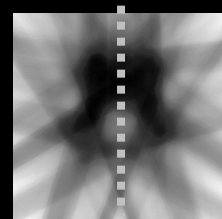
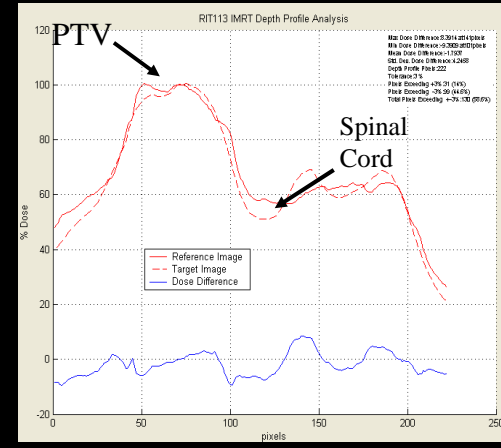
Doses must be recalculated in the same geometry that the measurement will be taken

Profile Analysis



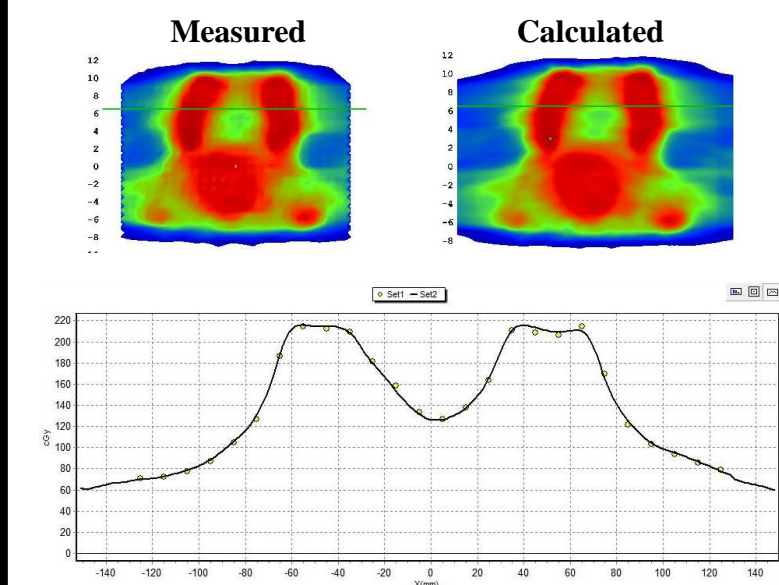
Using the profile tool, check the dosimetric agreement through the PTV and the Parotids

Profile Analysis

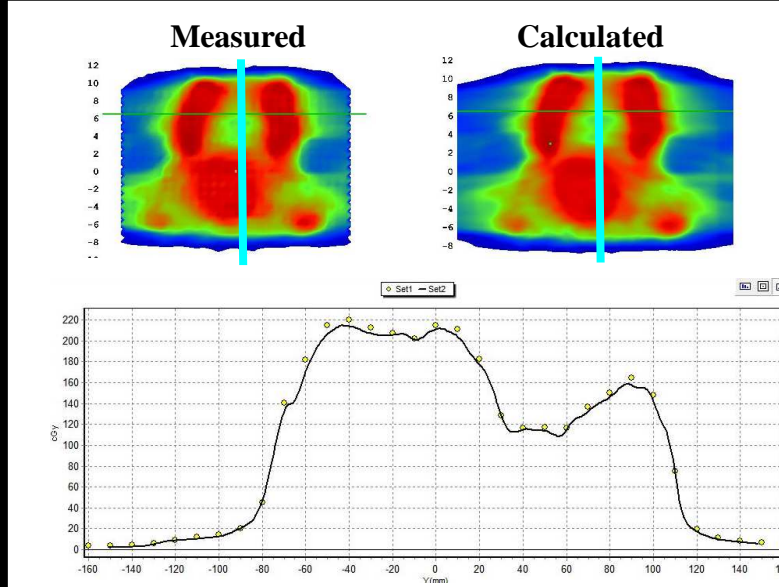


The worst dose error is typically found in dose wells, such as the spinal cord. Measure the dose error and make sure the spinal cord will not exceed the dose tolerance

Profile Analysis



Profile Analysis



Gamma Analysis

Measures the closest distance between each reference point and evaluated dose distribution after scaling by ΔD and Δd

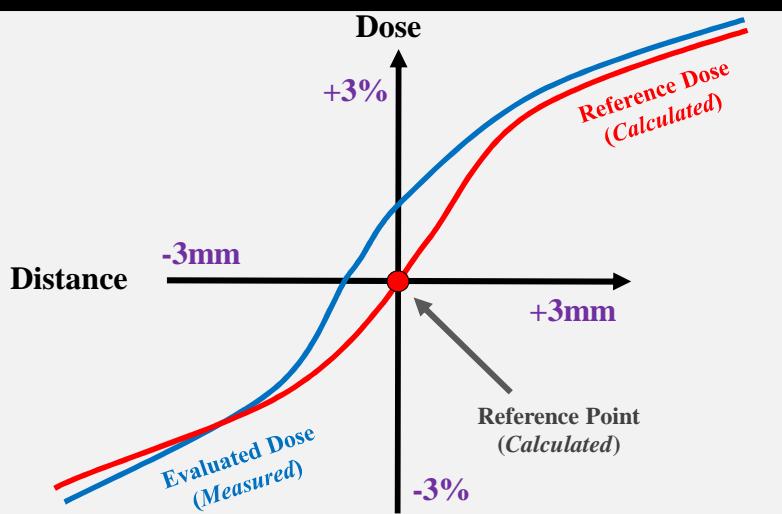
$$\Gamma(\vec{r}_e, \vec{r}_r) = \sqrt{\frac{r^2(\vec{r}_e, \vec{r}_r)}{\Delta d^2} + \frac{\delta^2(\vec{r}_e, \vec{r}_r)}{\Delta D^2}} \quad \gamma(r_r) = m \text{ in } \{\Gamma(\vec{r}_e, \vec{r}_r)\} \forall \{\vec{r}_e\}$$

- $r(\vec{r}_e, \vec{r}_r)$: spatial distance between evaluated and reference dose points
- ΔD : Dose difference criteria
- Δd : DTA

The point with the smallest deviation from reference point is a quantitative measure of the accuracy of the correspondence -> the quality index, γ (rr) of the reference point γ (rr) ≤ 1 -> correspondence is within the specified acceptance criteria

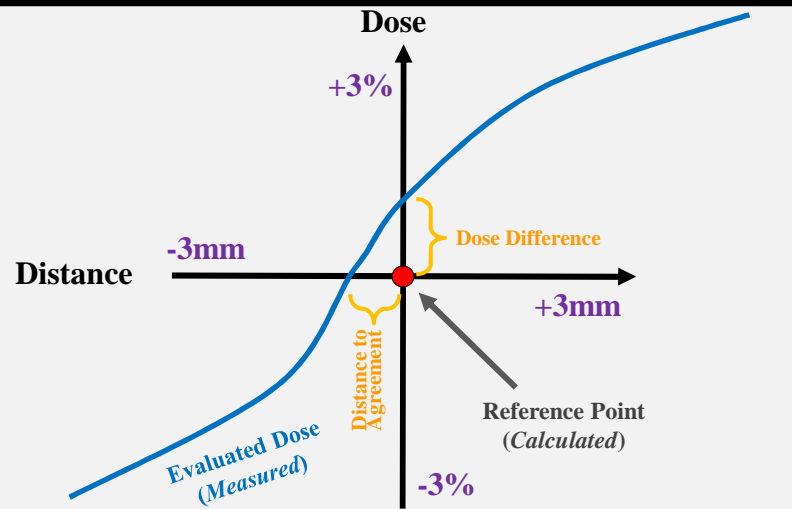
Low et al, Med Phys 30(9) 2455-64 (2003)

Gamma Analysis



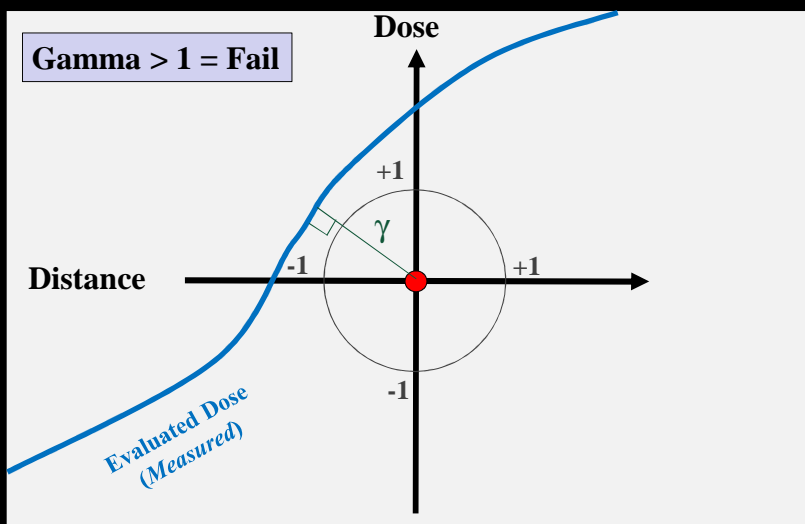
Low et al, Med Phys 30(9) 2455-64 (2003)

Gamma Analysis

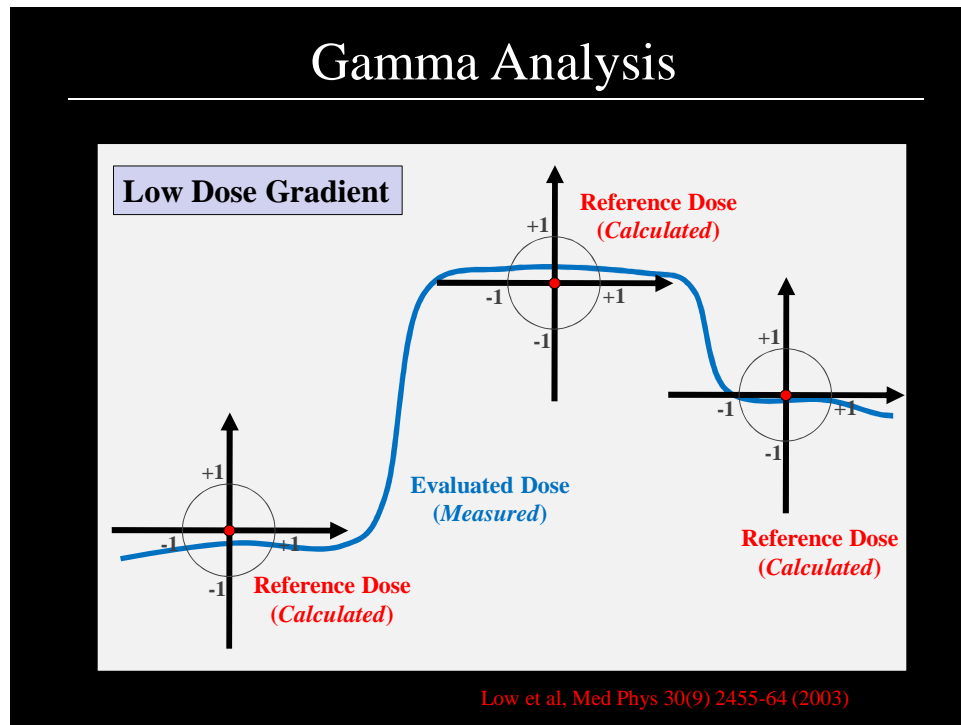
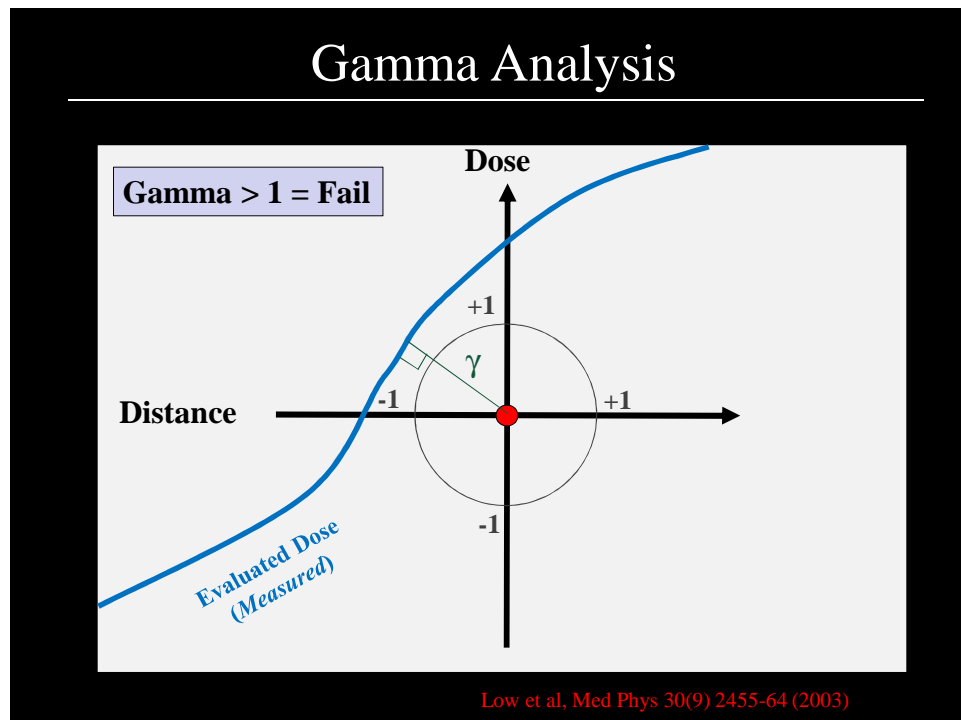


Low et al, Med Phys 30(9) 2455-64 (2003)

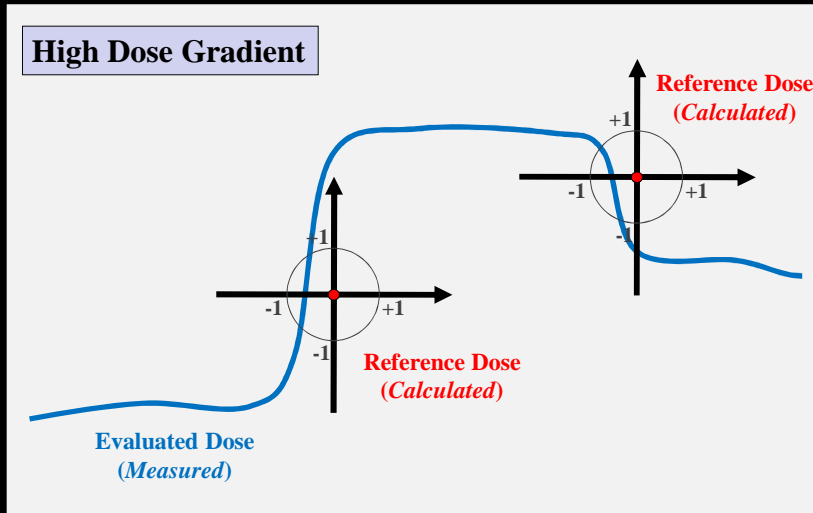
Gamma Analysis



Low et al, Med Phys 30(9) 2455-64 (2003)

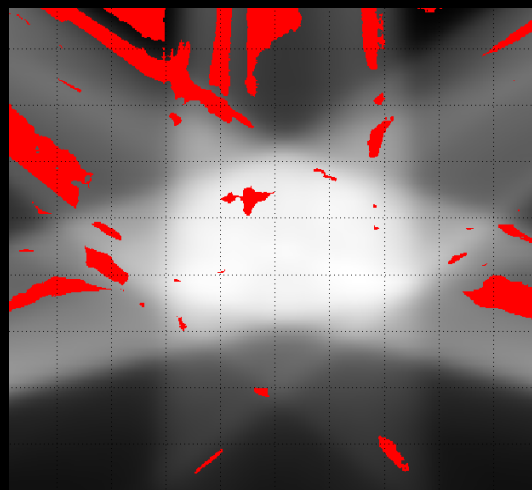


Gamma Analysis

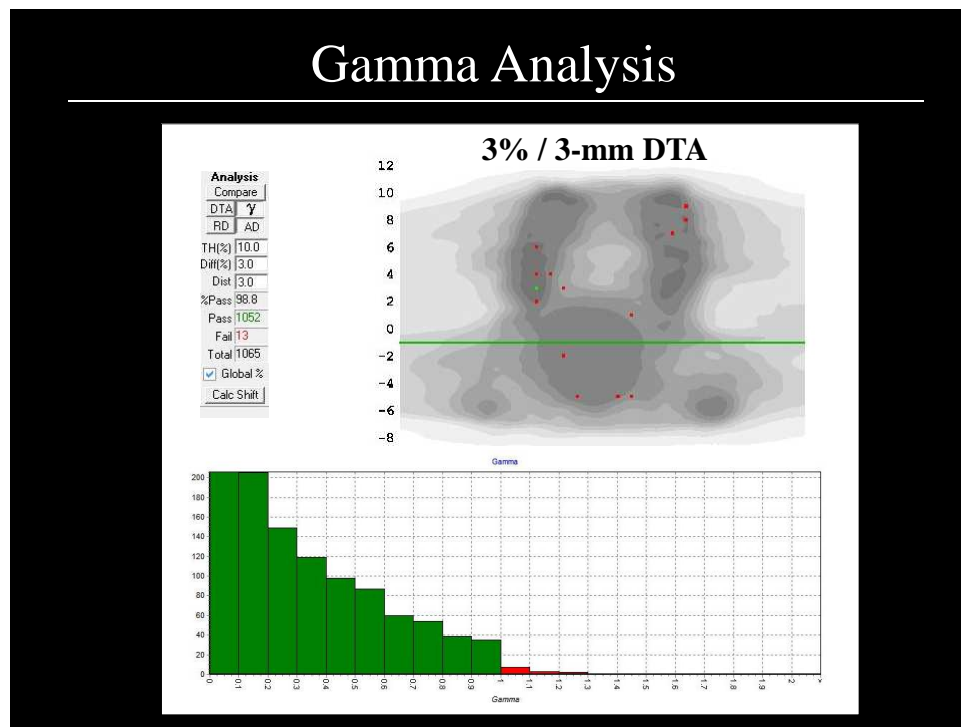
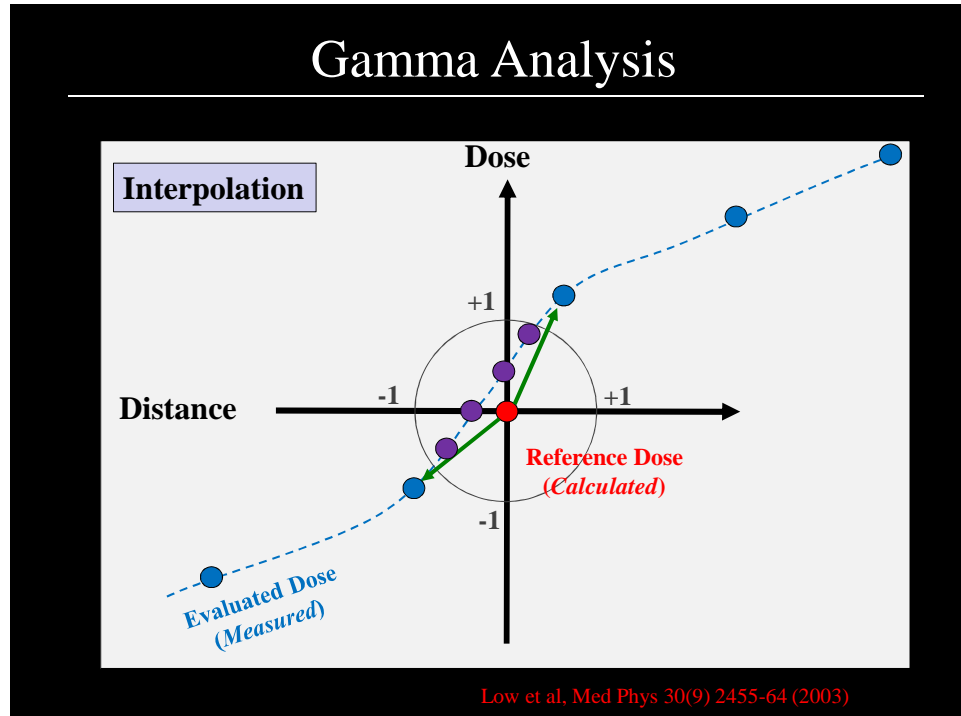


Low et al, Med Phys 30(9) 2455-64 (2003)

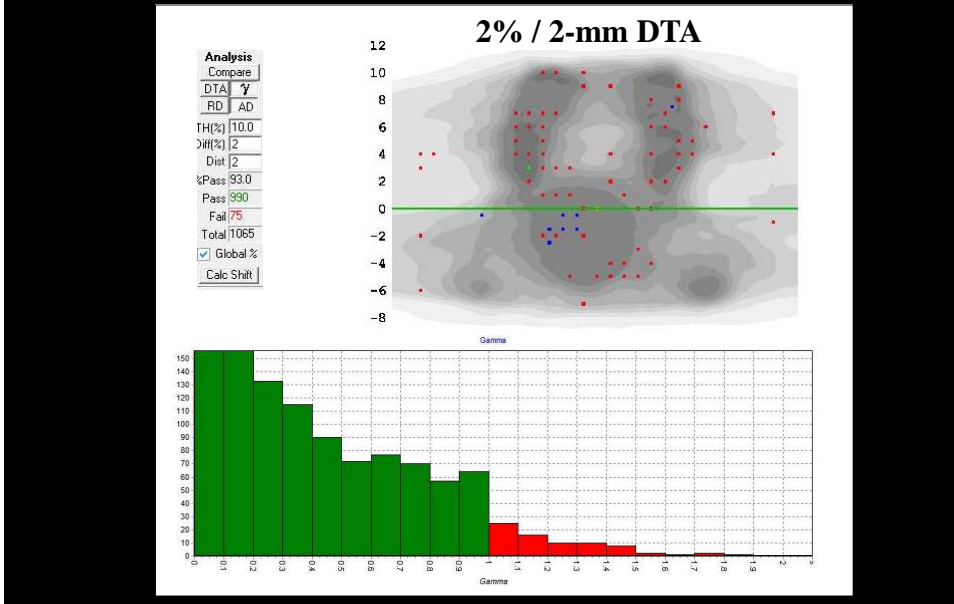
Gamma Analysis



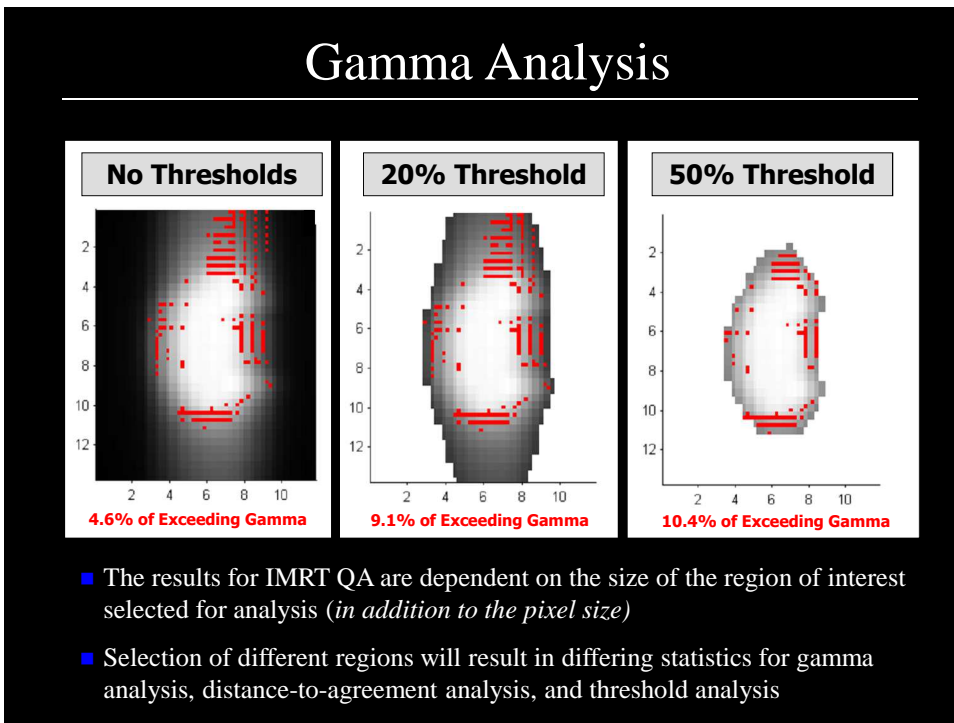
Red Pixels Exceed Gamma Index
(3%/3-mm DTA)



Gamma Analysis



Gamma Analysis



Radiographic Film for Patient Specific QA

Film Dosimetry

1826	Joseph Niepce	First Photograph
1836	J. M. Daguerre	Concept of developer
1889	Eastman Kodak	Cellulose nitrate base for emulsion
1890	Hurter &Driffield	Defined the term optical density
1895	Roentgen	First Radiograph
1896	Carl Schlussner	First glass plate for radiography
1913	Kodak	Film on Cellulose nitrate base
1918	Kodak	Double emulsion film
1933	Dupont	X-ray film with blue base
1942	Pako	Automatic film processor
1960	Dupont	Polyester base introduced
1965	Kodak	Rapid film processing
1972	Kodak	XTL and XV film for therapy
1983	Fuji	Computed radiography system
1994	3M	Dry process laser imaging

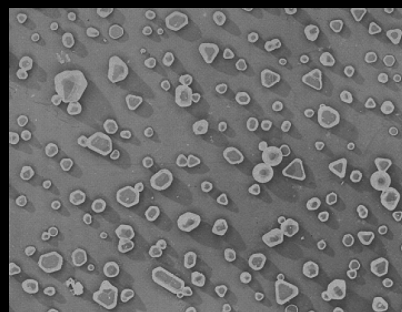
Film Dosimetry

Emulsion	20 μm
Base	200 μm
Emulsion	20 μm

There are 10^9 - 10^{12} grains/cm 2 grains/cm 2 in x-ray films

- Radiographic film consists of a transparent film base coated with an emulsion layer containing very small crystals of Silver halides (AgBr , AgI , AgCl , AgIAgI)
- When the film is exposed to ionizing radiation or visible light, a chemical change takes place within the exposed crystals
- This results in the formation of a latent image

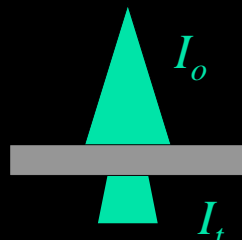
Film Dosimetry



Electron micrograph of grain in gelatin

- When the film is developed, the affected crystals are reduced to small grains of metallic silver
- The film is then “fixed”, and the unaffected gradually are removed leaving a clear film in their place
- The metallic silver is not affected by the fixer and causes darkening of the film
- The degree of blackening depends on the amount of silver deposited, and thus the dose

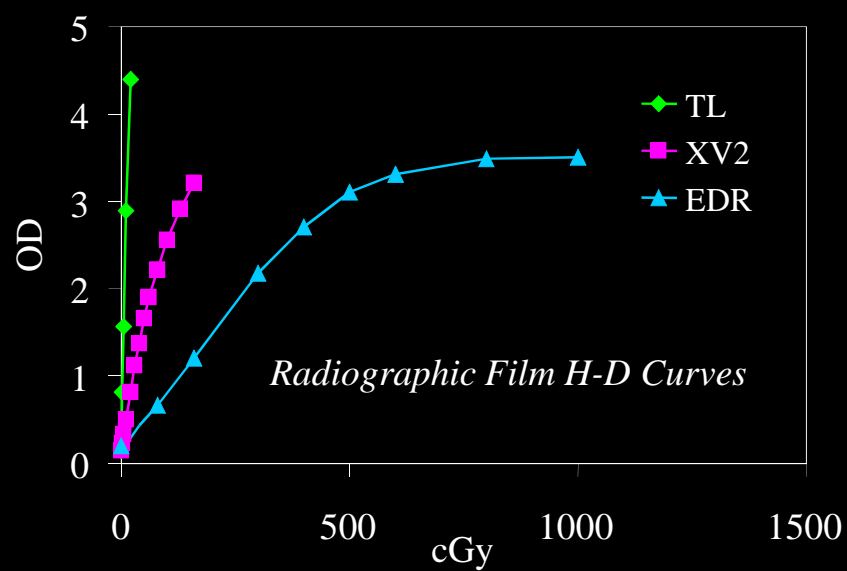
Film Dosimetry



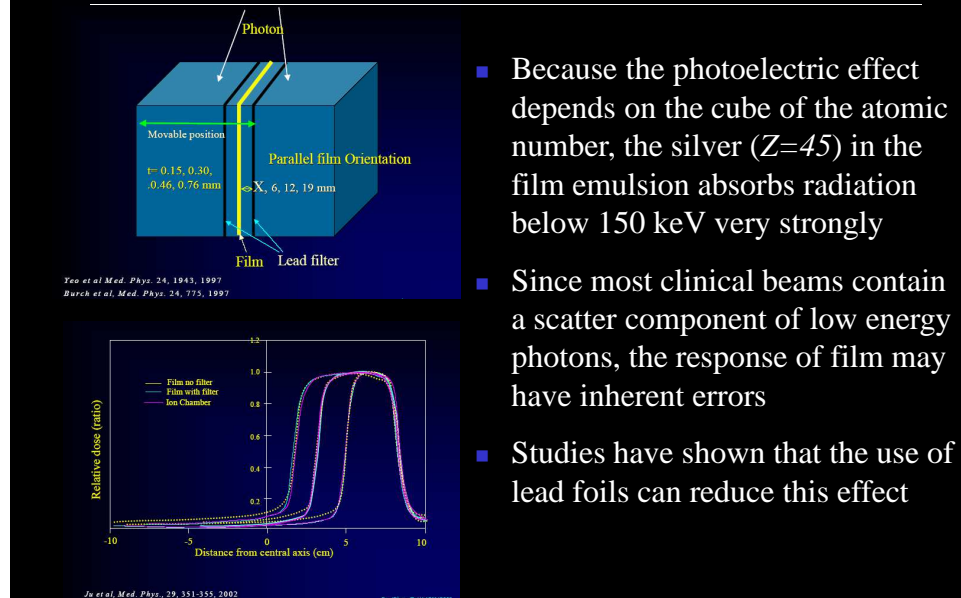
$$OD = \log \frac{I_o}{I_t}$$

- The degree of blackening of the film is measured by determining the optical density with a densitometry
- This instrument consists of a light source, a small aperture through which the light is directed, and a light detector
- A densitometer gives a direct reading of optical density if it has been calibrated using an ANSI standard strip

Film Dosimetry

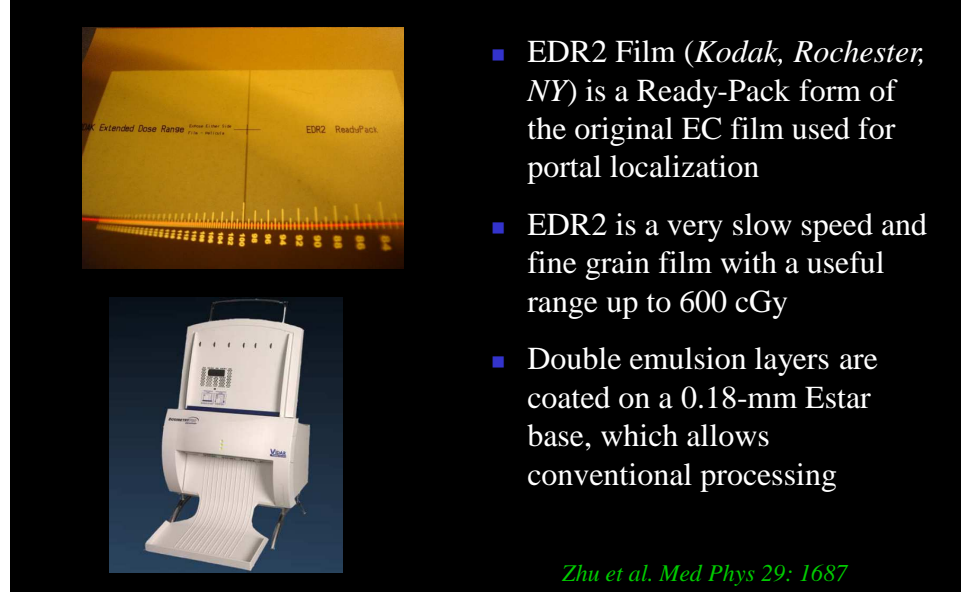


Film Limitations



- Because the photoelectric effect depends on the cube of the atomic number, the silver ($Z=45$) in the film emulsion absorbs radiation below 150 keV very strongly
- Since most clinical beams contain a scatter component of low energy photons, the response of film may have inherent errors
- Studies have shown that the use of lead foils can reduce this effect

Film Calibration



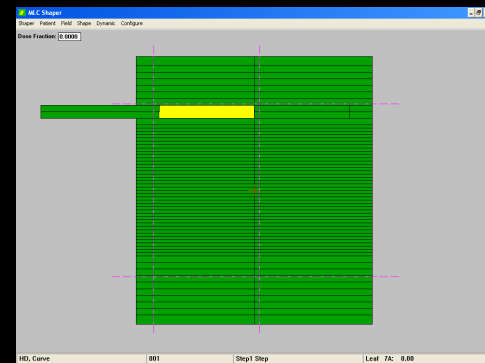
- EDR2 Film (*Kodak, Rochester, NY*) is a Ready-Pack form of the original EC film used for portal localization
- EDR2 is a very slow speed and fine grain film with a useful range up to 600 cGy
- Double emulsion layers are coated on a 0.18-mm Estar base, which allows conventional processing

Zhu et al. Med Phys 29: 1687

Film Calibration

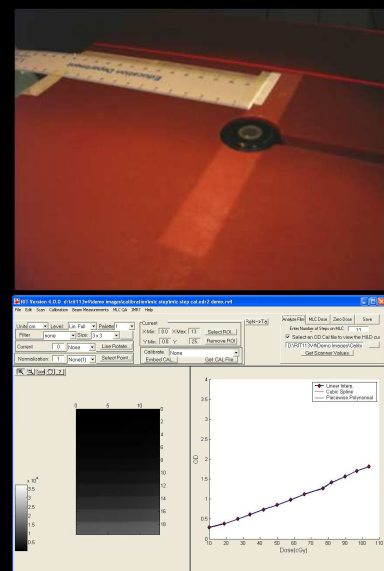
- A 13 step calibration film can be generated using a dMLC step-and-shoot file
- Each stripe delivers a progressively lower dose
- Easier than using square films

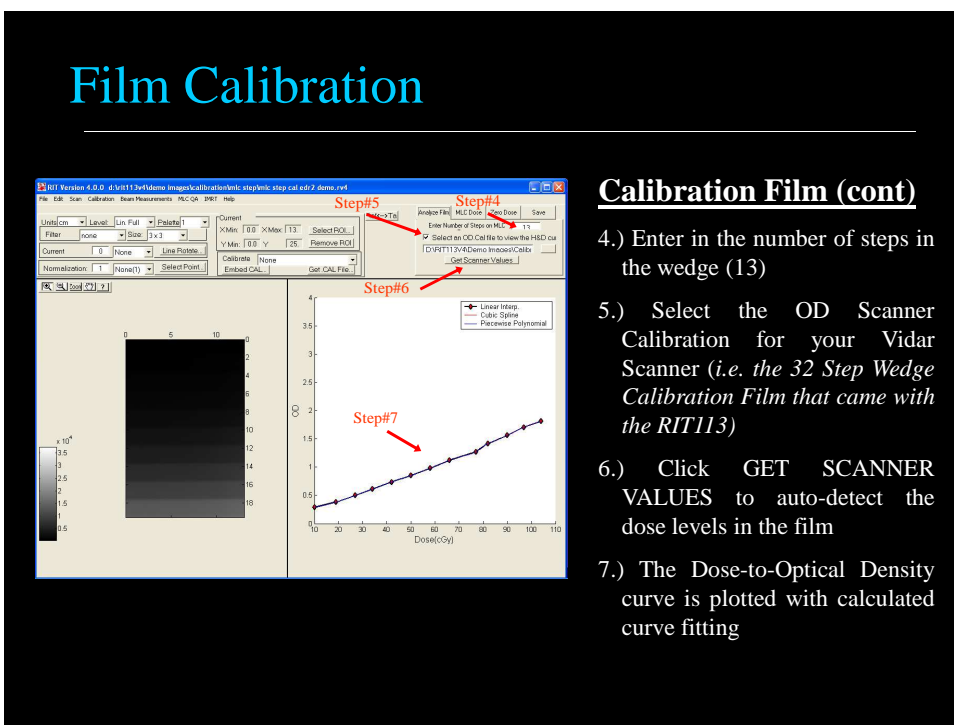
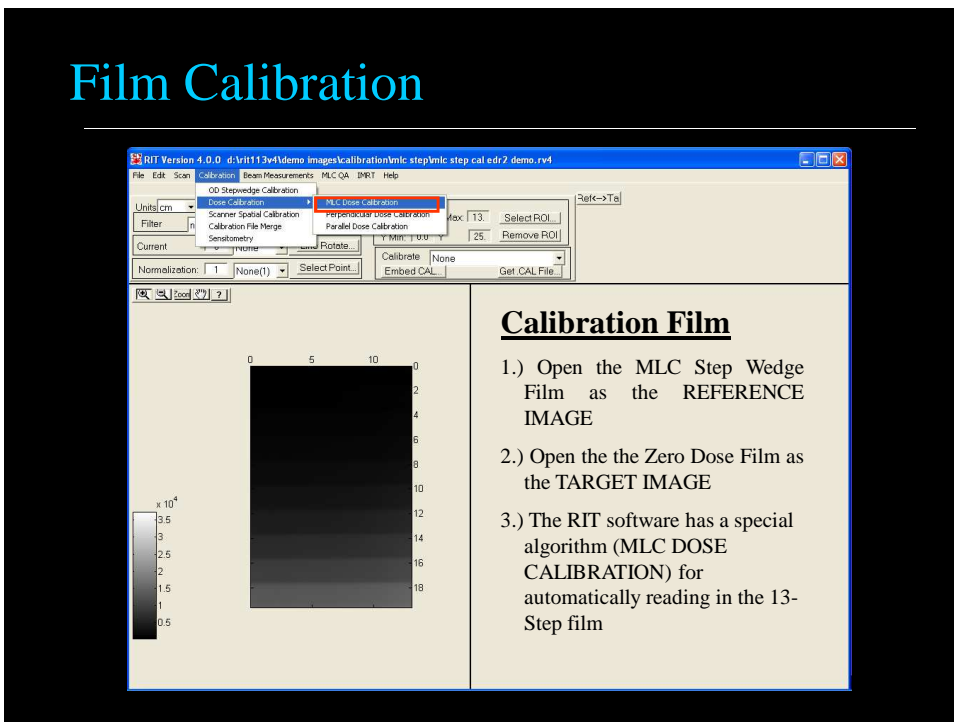
96.1 cGy
93.4 cGy
87.1 cGy
79.8 cGy
72.4 cGy
65.1 cGy
57.3 cGy
49.6 cGy
41.8 cGy
34.0 cGy
26.1 cGy
18.2 cGy
10.4 cGy



Film Calibration

- The dose must be measured in each of the 13 stripes using an ionization chamber
- Place a water equivalent phantom at isocenter
- Align the chamber in the center of the first 2-cm wide stripe
- Move the couch longitudinally 2 cm to move the chamber to the next stripe
- Scan the film into a dosimetry package and create a dose-to-density curve



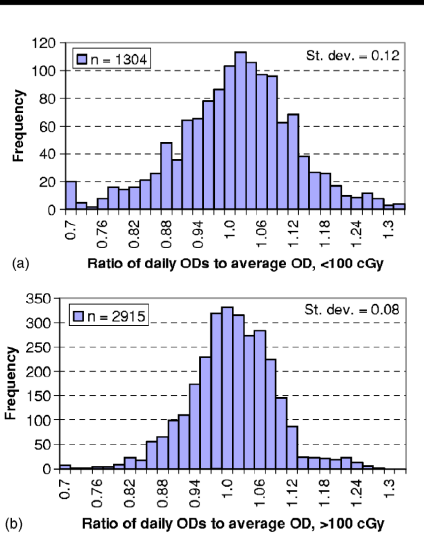


Radiographic Film

- The single greatest disadvantage for radiographic film is the requirement for wet processors, which are rapidly disappearing from hospitals



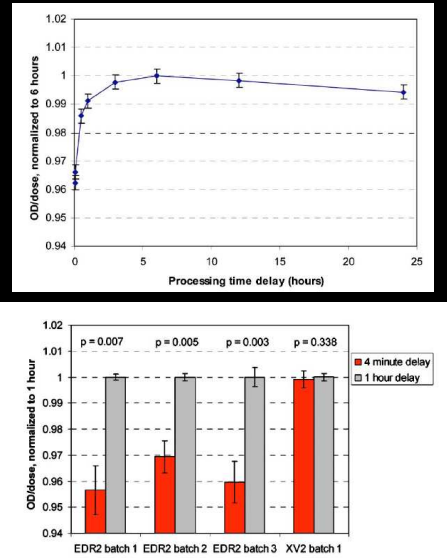
Radiographic Film



- Calibration variations have been studied over an 18 month time period (*547 individual calibration films*)
- Large standard deviations have been observed in film calibration
- These observed differences are likely due to the variation over time in the film processor properties (*temperature, chemical age, etc...*)

Childress et al. Med Phys 32: 539

Radiographic Film

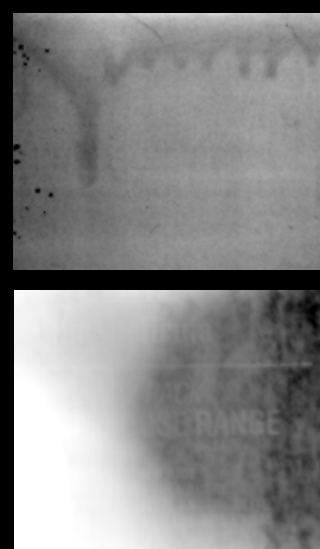


- The amount of time between exposure and processing alters Kodak EDR2 film's absolute dose response
- If calibration films are exposed following patient QA, and all films are processed together, the time delay for the calibration would be shorter
- The film was within 1% of its stable values after 1 hour, and within 2% after 30 min

Childress et al. Med Phys 31:2284

Radiographic Film

- Incorrect processor chemistry, temperature, and roller maintenance can cause artifacts on EDR Film
- These problems become more frequent when large volume processors are used exclusively by physics
- Another problem can come from the Ready-Pack jackets, which are not entirely light-proof



Film Registration

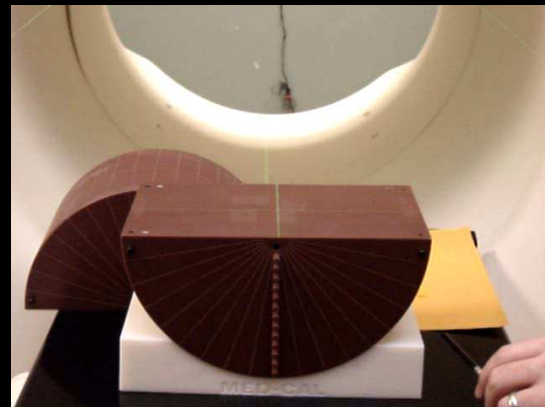
- The phantom is placed on the treatment and aligned with the in room lasers
- Ion Chamber(s) are used to measure absolute dose prior to the first treatment
- Film is used to measure the shape of the dose distribution



Solid Water Phantom with Farmer Chamber

Film Registration

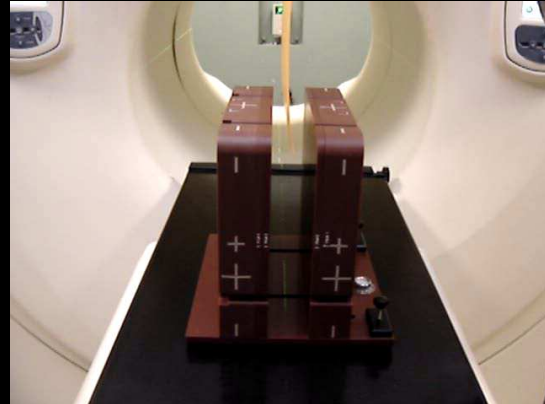
- The phantom is placed on the treatment and aligned with the in room lasers
- Ion Chamber(s) are used to measure absolute dose prior to the first treatment
- Film is used to measure the shape of the dose distribution



Cylindrical Phantom with Small Volume Chamber

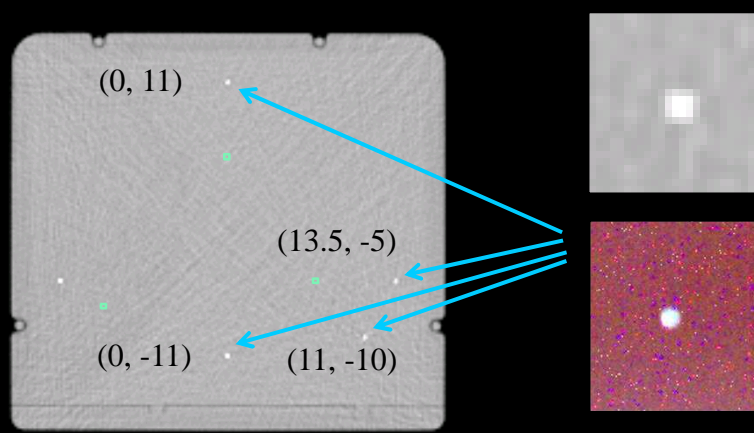
Film Registration

- The phantom is placed on the treatment and aligned with the in room lasers
- Ion Chamber(s) are used to measure absolute dose prior to the first treatment
- Film is used to measure the shape of the dose distribution



Med-Tec Phantom with Small Volume Chamber

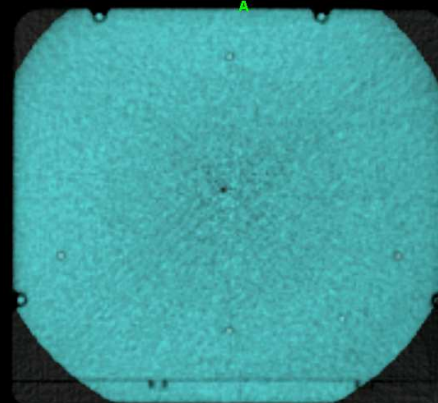
Film Registration



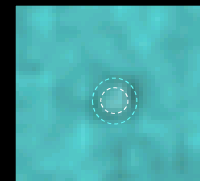
Metal Pins

The Film is marked at know locations by metal pins that are built into the phantom

Film Registration



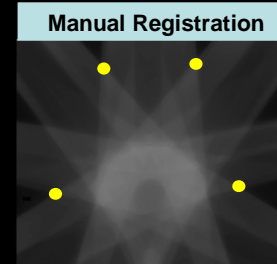
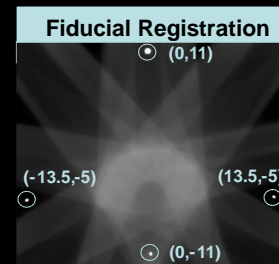
MVCT kVCT



CT Images are acquired of the phantom and the metal pins are aligned with the planning CT image

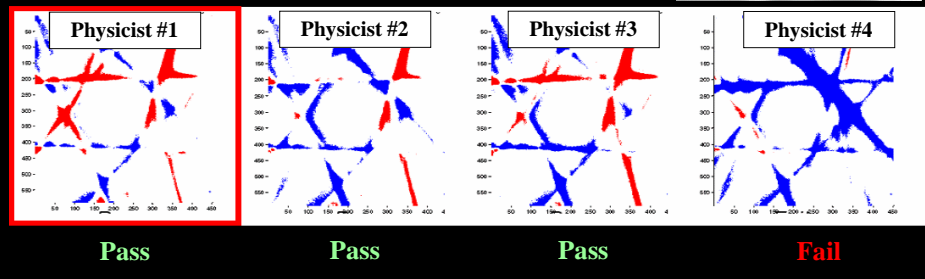
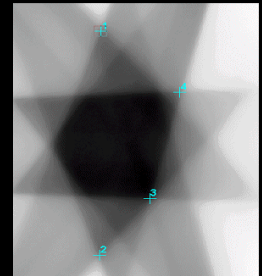
Film Registration Techniques

- In radiochromic film based IMRT QA, the film must be registered with the calculated doses
- Fiducial based Registration
 - Film physically marked relative to isocenter
 - Film is marked, a template is created, and the plan is registered to the film by matching points
- Manual based Registration
 - Common points selected on both film and plan by visual examination

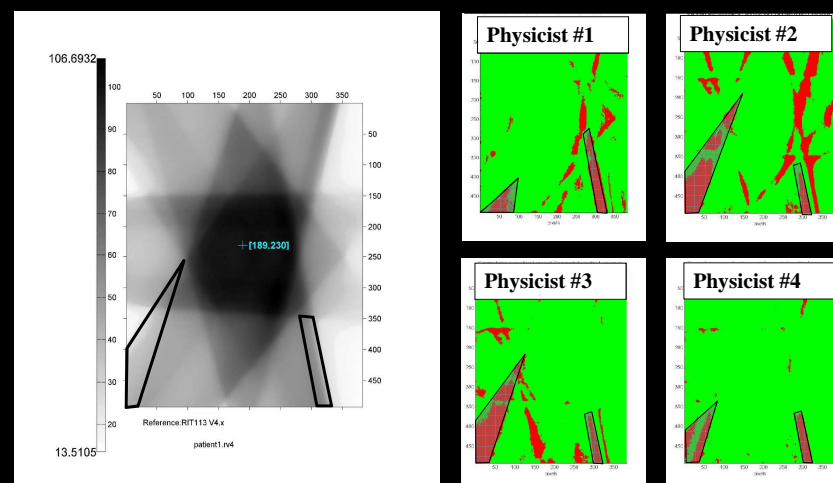


Manual Registration

- Without fiducial marks on the film, users place registration points in unique locations
- This yields different results from inter- and intra-user variations
- In this example, four physicists performed manual registration of the same film using a ± 3 dose threshold analysis to determine if the QA passed or failed

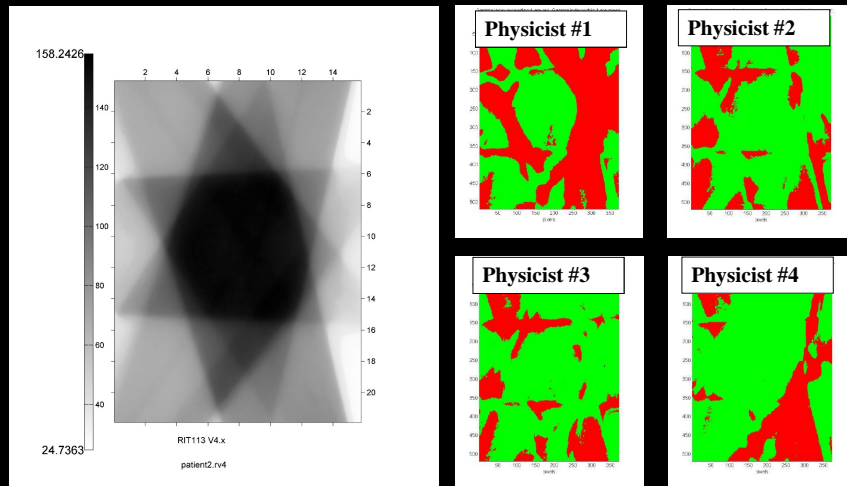


True Pass



- Gamma ($3\% / 3\text{-mm}$) analysis for a prostate case that had a 100% pass rate
- Dose discrepancy occurred outside the PTV in the low dose region

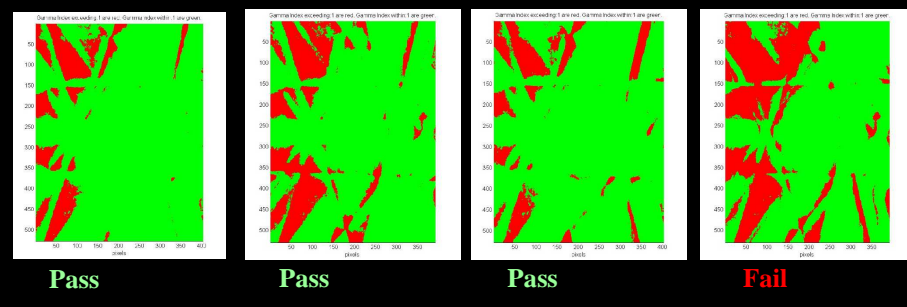
True Failures



- Gamma (3%/3-mm) analysis for a prostate case that had a 100% failure rate
 - Dose discrepancy occurred in the gradient (*Rectal*) and low dose regions

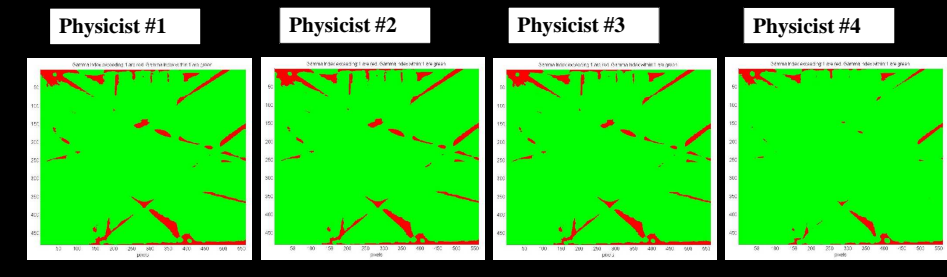
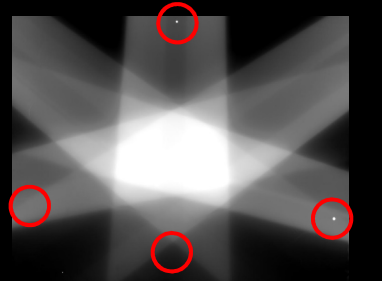
Intra-User Variations

- Two of the cases in the test data set were the same film
 - These two cases were used to evaluate intra-user variation in film analysis
 - Below is an example of a gamma pass/fail analysis performed by the same physicist over a period of 6 months
 - There can be significant intra-user variation in the analysis depending on the position of the manual registration points and the normalization point



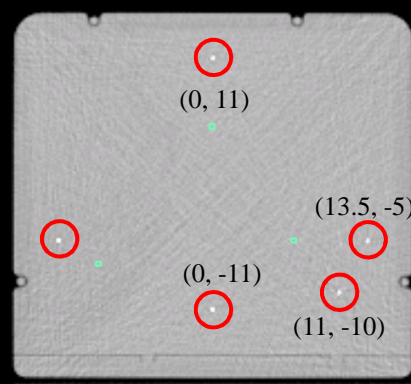
Fiducials

- The addition of known fiducial points in the phantom greatly reduced inter-and intra-users variation
- In this example, the variation between physicists using the gamma analysis ($3\% / 3\text{-mm DTA}$) is almost negligible



Fiducial Registration

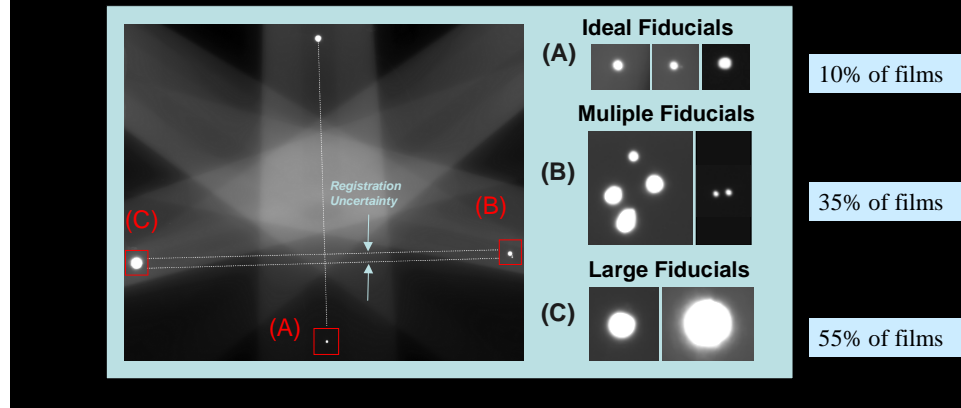
- In fiducial based registration, the film and the phantom are positioned relative to isocenter
- The films are then marked at known locations relative to isocenter
 - Pins or Metal Markers are Built-into certain IMRT Phantoms*
 - Pins or Pens can be used to manually mark the film*
- The resulting fiducial marks on the film provide a measure of the correct placement of dose



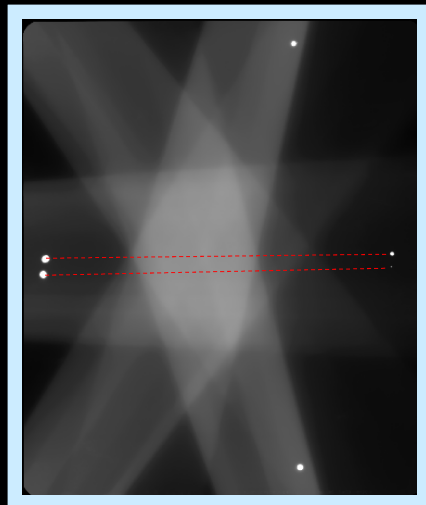
CIVCO Benchmark™
IMRT QA Phantom

Fiducial Registration

- Fiducial based registration is subject to user errors (*especially with radiographic film*) if not used correctly
- In a review of IMRT QA films irradiated in multiple IMRT phantoms, only 10% of the films had single small fiducial marks



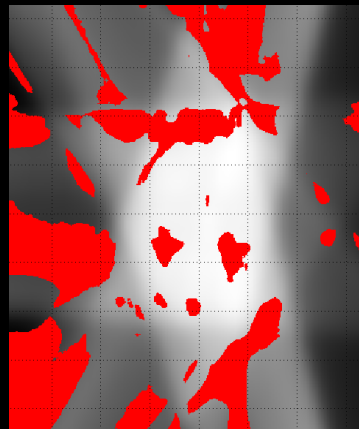
Fiducial Registration



- Multiple fiducial marks occurred in 35% of the IMRT QA films due to
 - Manual Double Pricking
 - Film moving inside a phantom with built-in pins
- Having multiple fiducials makes it difficult to obtain a correct film-to-plan registration
- In this example, an axial prostate film has upper and lower fiducial marks
- These errors can be entirely eliminated with correct film placement

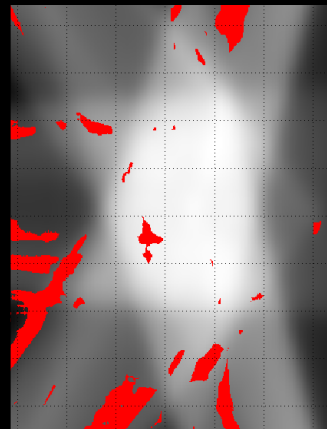
Fiducial Registration

Lower Points Selected



22% of pixels exceeding gamma index (3%/3-mm DTA)

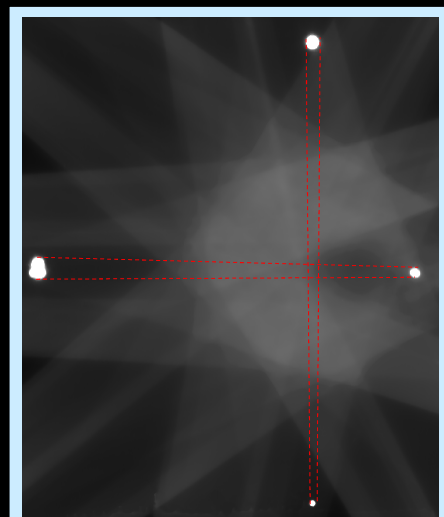
Upper Points Selected



9% of pixels exceeding gamma index (3%/3-mm DTA)

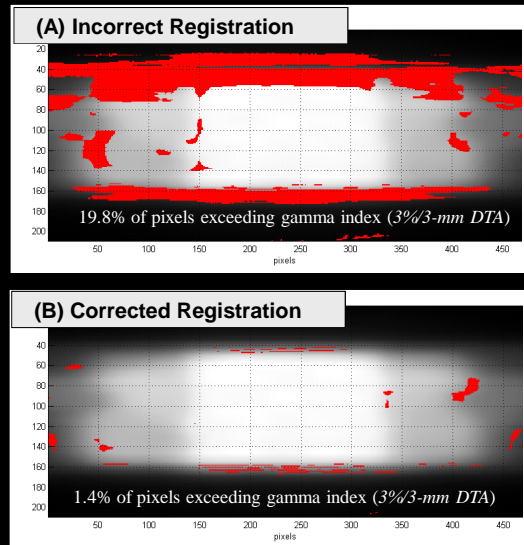
Fiducial Registration

- Large fiducials occurred in 55% of the IMRT QA films
- The goal of pricking the film is to lightly score the film, not to push the pin completely through
- Light will leak through the fiducial holes in the Ready-Pack jacket
- Having very large fiducials present also makes it difficult to obtain a correct registration
- These errors can be entirely eliminated with careful film marking and storage of the film in a dark area prior to processing



Registration Uncertainty

- Another source of error is unintentional rotation of the film after the registration marks have been made
- This will result in a misalignment between the dose on the film and the calculated doses
- Rotation errors occurred in 30% of irradiated IMRT QA films
- This incidence of this type of error can be minimized by simply taping the film to the phantom



QA Analysis (*All Techniques*)

- In this example, the percent of pixels exceeding a gamma threshold of 1 are reported for 18 patients
- Gamma histogram results can be easily skewed by increasing the size of the analysis region of interest to include more of the low-dose low-gradient region
- It is important when selecting a threshold for pass/fail, that the region of interest is consistent

Percent of Pixels Exceeded a Gamma Threshold of 1 (3%/3-mm DTA) for Different Dose Thresholds

Patient	Dose Threshold for Analysis					
	0%	10%	20%	30%	40%	50%
1	3.1	3.1	1.8	1.5	1.5	1.6
2	4.7	2.7	2.8	2.4	3.0	3.0
3	6.7	6.7	6.2	5.5	5.7	5.0
4	1.9	3.3	4.4	5.3	5.9	5.7
5	6.1	8.8	9.2	7.2	7.2	7.4
6	4.7	7.8	9.3	9.8	8.4	8.1
7	15.8	19.6	19.2	15.7	12.5	9.1
8	8.1	10.0	10.8	11.5	10.4	9.7
9	4.0	6.2	7.1	9.1	9.1	10.1
10	4.6	8.0	9.1	10.5	10.8	10.4
11	17.5	17.7	15.9	13.3	12.3	10.7
12	5.1	8.8	10.7	11.5	13.0	11.7
13	11.4	14.9	13.1	11.5	13.4	12.8
14	15.2	14.6	14.2	14.4	13.3	13.3
15	6.9	12.8	16.4	15.6	14.7	14.0
16	4.2	5.5	9.4	14.6	15.4	15.1
17	10.4	10.1	12.1	15.3	16.2	16.3
18	11.4	12.4	14.3	14.8	16.9	18.2
Average	7.9	9.6	10.3	10.5	10.5	10.1
SD	4.7	4.9	4.8	4.5	4.5	4.5

Radiochromic for Patient Specific QA

Radiochromic Film

- Radiochromic film is an alternative to radiographic film for facilities without a wet processor
- It is nearly tissue-equivalent and does not require a processor for generating the optical density response to ionizing radiation
- Furthermore, the film has been designed to be handled in interior room light
- Radiochromic film for IMRT QA comes in two types (*EBT* and *EBT2*) from International Specialty Products

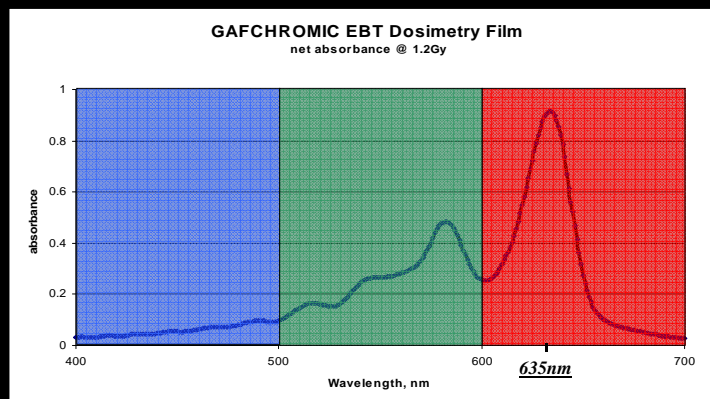


Radiochromic Film

Radiology/diagnostic	Energy Range	Dose Range
GAFCHROMIC® XR- R	kilovolt	0.1Gy to 15 Gy
GAFCHROMIC® XR-CT	kilovolt	0.1cGy to 50 cGy
GAFCHROMIC® XR- QA	kilovolt	0.1cGy to 20 cGy
Radiotherapy	Energy Range	Dose Range
GAFCHROMIC® HD-810	megavolt	5Gy to 500Gy
GAFCHROMIC® MD-55	megavolt	1Gy to 100Gy
GAFCHROMIC® HS	megavolt	0.5Gy to 40Gy
GAFCHROMIC® RTQA	megavolt	0.02Gy to 8Gy
GAFCHROMIC® EBT**	megavolt	0.02Gy to 8Gy

Courtesy of ISP

Spectral Response



- When the active component is exposed to radiation, it reacts to form a blue colored polymer with absorption maxima at about 635 nm and 585 nm
- The film can be measured with transmission densitometers, film scanners or spectrophotometers

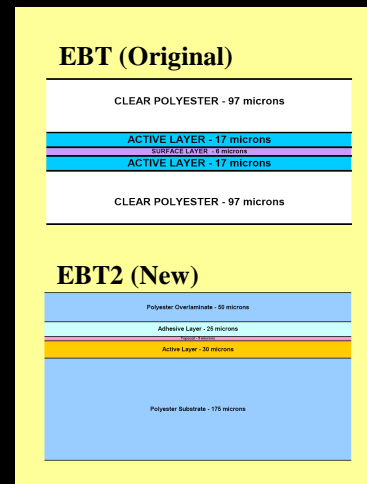
Radiochromic EBT Film

- The original EBT radiochromic film is made by laminating two separate films
- Each film has an active layer 17 μm thick and a surface layer 3 μm thick
- The coatings are applied to a transparent 97 μm thick polyester
- The product is formed by laminating the two pieces of film together using a technique requiring no intermediate adhesive layer



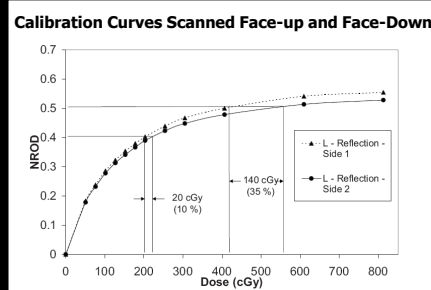
Radiochromic EBT2 Film

- EBT2 is made by combining a clear polyester over-laminate with the active film coating
- The over-laminate consists of a 50 micron polyester
- The substrate of the active film is a clear 175 micron polyester that coated with a 30 microns active layer film and a 5 microns topcoat
- The over-laminate and the substrate are bonded together with approximately 25 microns of pressure-sensitive adhesive
- Whereas the EBT film was symmetric front-to-back, the new EBT2 film is not symmetric

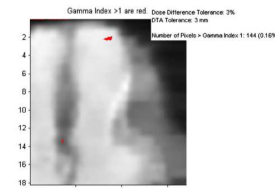


Radiochromic: Face-Up / Face Down

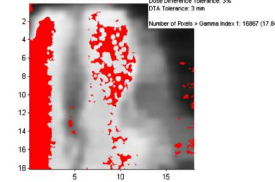
- Desroches, Bouchard, and Lacroix (*Med Phys* 37, April 2010) have reported optical density difference between scanning the EBT2 “face up” or “face down”
- The authors demonstrate potential errors of 17.8% by inverting the film scanning side on the gamma index for 3%/3-mm criteria



Calibration Curve Side 1 with Film Scanned on Side 1



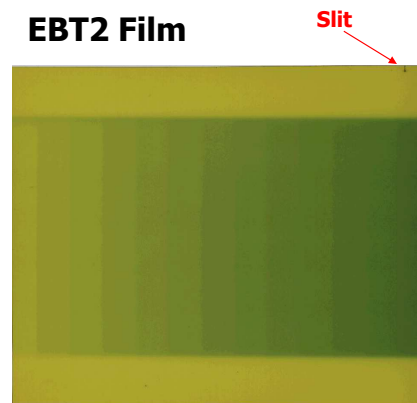
Calibration Curve Side 2 with Film Scanned on Side 1



Radiochromic: Face-Up / Face Down

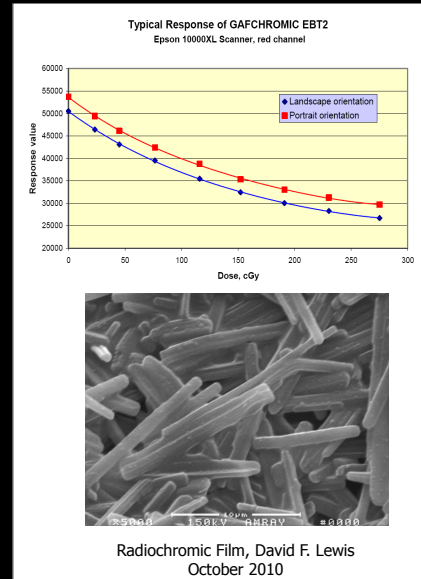
- The manufacturer cuts a small slit along one edge to assist in determining which side is which
- In addition, the 175 μm polyester base is smooth and the 50 μm polyester laminate is textured
- Place the film so that the 175 micron polyester base is facing the glass window on the bed of the scanner
- Position the film in the landscape orientation so that the manufacturer's slit marking is in the top right corner

EBT2 Film



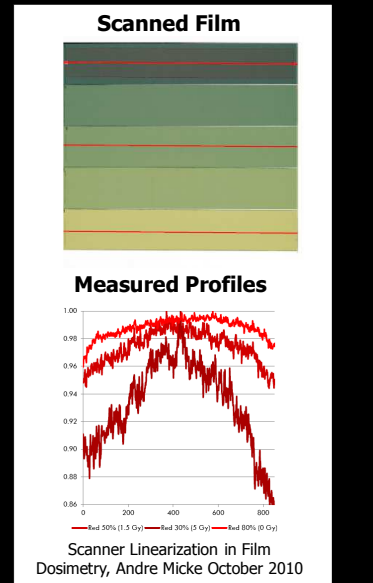
Radiochromic: Orientation

- Vidar, Epson, and Microtek CCD scanners utilize an extended light source and the sensor has a linear array of detectors
- When radiochromic film is digitized, the response is sensitive to the orientation of the film on the scanner
- The response difference is the result of anisotropic light scattering off the needle-like particles in the active layer
- These particles tend to align with their long axes parallel to the coating direction they scatter light differently in orthogonal directions



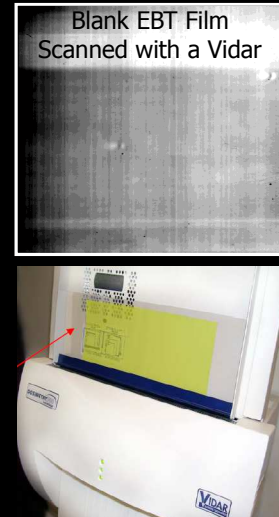
Radiochromic: Lateral Scanner Effect

- The response of scanners is not flat over of their scan field
- Lateral scanner non-linearity depends on dose, film uniformity, and noise
- These non-uniformities are most prominent within about 2-3 cm of the left and right sides of the scanner
- It is critical to always scan EBT2 films in the same orientation
 - Place the film in the center of the scanner using a template
 - Scan in landscape mode with the short dimension of the film parallel to the long dimension of the scan bed



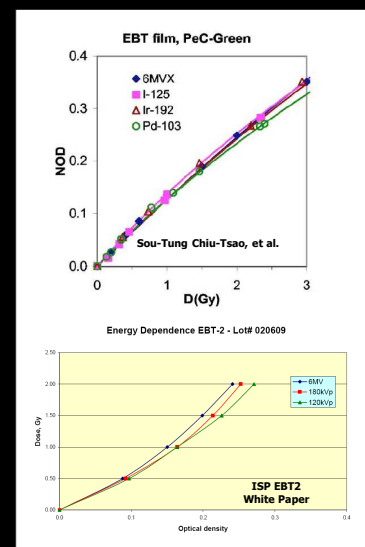
Radiochromic: Contrast Banding

- Vidar scanners can produce “contrast bands” across the digitized images from flexing of the film
- ISP recommends putting the film in a clear plastic sleeve to eliminate these bands
- The sleeve is 14” long and extends about 2” beyond the leading and trailing edges of the film
- Maintains the film in a single plane in front of the slit thus preventing the banding



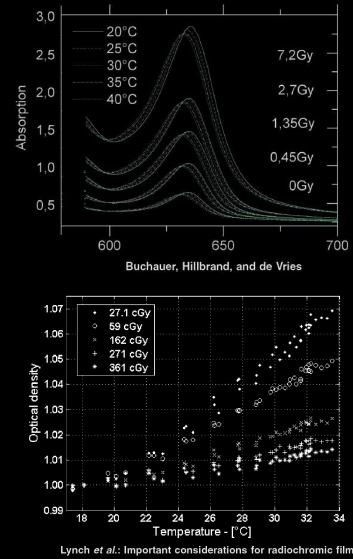
Radiochromic: Energy Dependence

- The energy response of EBT and EBT2 films has been reported in *Medical Physics*
- Sou-Tung Chiu-Tsao found that the EBT film response is nearly independent of radiation energy
- In a more recent study, Lindsay et al reported an energy dependence at 105 kV
- The authors indicated that differences in energy response of EBT and EBT-2 films were due to changes in the chemical composition of the film
- ISP is optimizing the manufacturing process to minimize or eliminate this effect



Radiochromic: Temp Dependence

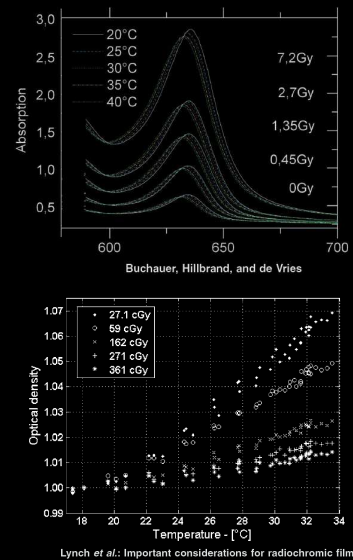
- Temperature dependent readout deviations can arise from different temperatures between scanning the calibration curve and scanning the patient's QA film
- An increase in temperature can lead to a dose error if scanner temperature is not constant
- Lynch et al. reported a magnitude of 0.5% readout increase per $^{\circ}\text{C}$, and Buchauer et al reported a $1\%/\text{ }^{\circ}\text{C}$ increase
- The change appears to be reversible as the temperature decreases



Radiochromic: Temp Dependence

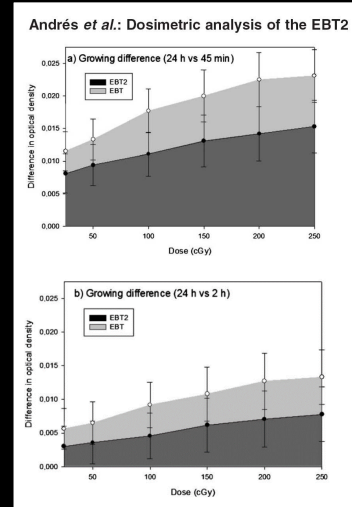
Temperature Control

- Turned on the scanner at least 30 min before measurements
- Perform five preview scans without film on the scanner bed in order to warm-up the scanner lamp
- Make sure that the temperature in the scanner is the same as when the calibration curve was created
- Limit the number of the number of consecutive scans so that the temperature during scanning is not significantly increased



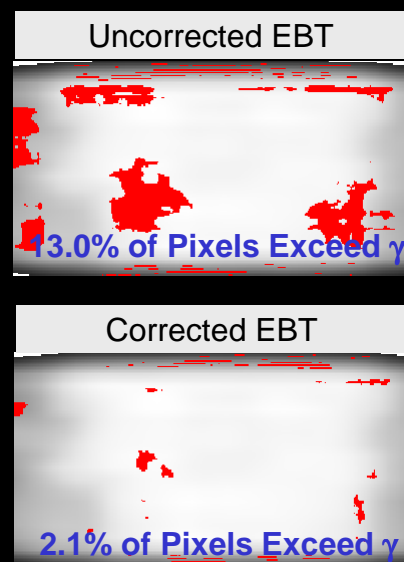
Radiochromic: Time Dependence

- Andres et al. studied optical density changes in radiochromic film increases following exposure (*Med Phys* 37, December 2010)
- They reported that EBT2 film increased in optical density by 6%, and EBT increased 8% over 24 hours
- This is a major issue when obtaining absolute doses from the film
- For absolute dosimetry, wait at least 2 hours for EBT2 and 6 hours for EBT film to allow for image stabilization



Radiochromic: Background Subtraction

- There are two methods for correcting for the non-uniformities:
 - Scan the film prior to irradiation and use the image as a background/baseline image
 - Use the Blue Channel on the irradiated film as a background/baseline image
- In order to use EBT film, the analysis software must be capable of correcting each piece of film
- In this example, calculated and measured doses are shown for uncorrected and corrected EBT film scanned with a Vidar VXR-16



Heterogeneous IMRT Phantoms

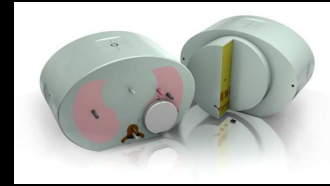
IMRT Phantoms

- Patient specific IMRT QA is traditionally delivered using a homogenous phantom
- These measurement on a homogenous phantom are being used to evaluate plan acceptability
- However, patients are very heterogeneous
- This has the potential to hide treatment planning calculation errors



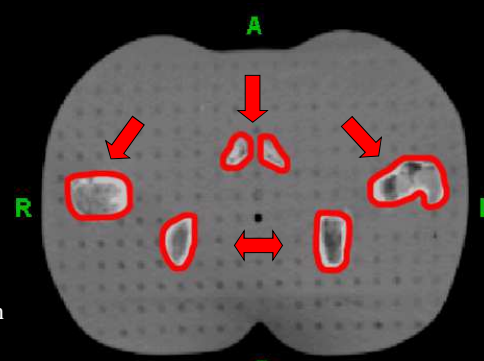
Heterogenous Phantoms

- Measurements can also be performed in heterogeneous phantoms
- One such phantom is the RANDO phantom
 - Slices contain a natural human skeleton cast inside material radiologically equivalent to human soft tissue
 - Lung portion of phantom made with lower density material simulating human lungs in median respiratory state



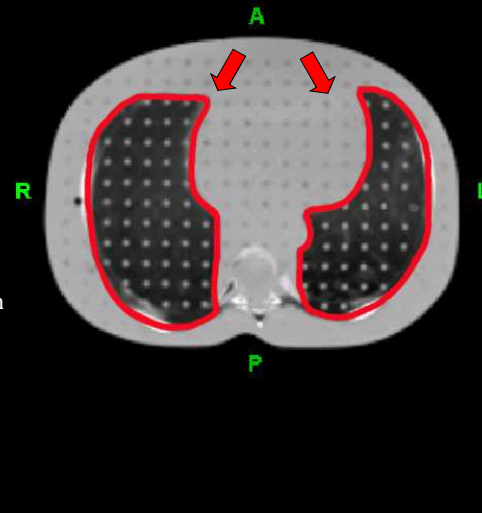
RANDO Phantoms

- Measurements can also be performed in heterogeneous phantoms
- One such phantom is the RANDO phantom
 - Slices contain a natural human skeleton cast inside material radiologically equivalent to human soft tissue
 - Lung portion of phantom made with lower density material simulating human lungs in median respiratory state



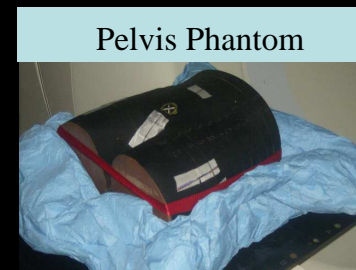
RANDO Phantoms

- Measurements can also be performed in heterogeneous phantoms
- One such phantom is the Rando phantom
 - Slices contain a natural human skeleton cast inside material radiologically equivalent to human soft tissue
 - Lung portion of phantom made with lower density material simulating human lungs in median respiratory state



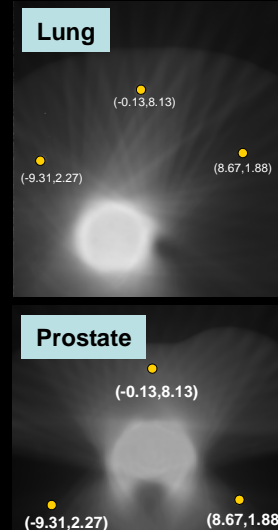
RANDO Phantoms

- Phantom is typically divided into separate sections
 - Lung phantom-slices 14 to 19
 - Pelvis phantom-slices 26 to 35
- Phantom position in Vac-Loks
- Treatment plans for actual patients copied and re-calculated on the Rando
 - Convolution/Superposition beamlet based dose calculation



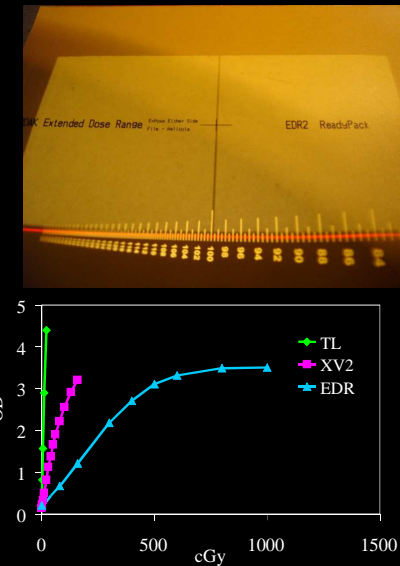
RANDO Phantoms

- QA plans designed so tumor volume from patient resided in same anatomical site inside anthropomorphic phantom
- Used Kodak radiographic EDR2 placed transversely between two phantom slices
- Film taped to inside surface of phantom preventing movement
- Marked in three locations relative to machine isocenter



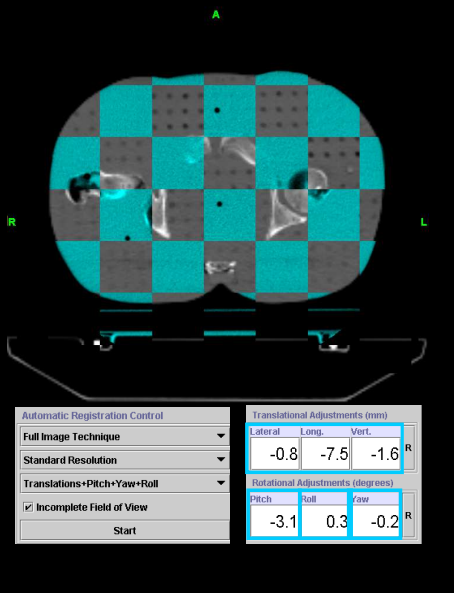
RANDO Phantoms

- QA plans designed so tumor volume from patient resided in same anatomical site inside anthropomorphic phantom
- Used Kodak radiographic EDR2 placed transversely between two phantom slices
- Film taped to inside surface of phantom preventing movement
- Marked in three locations relative to machine isocenter



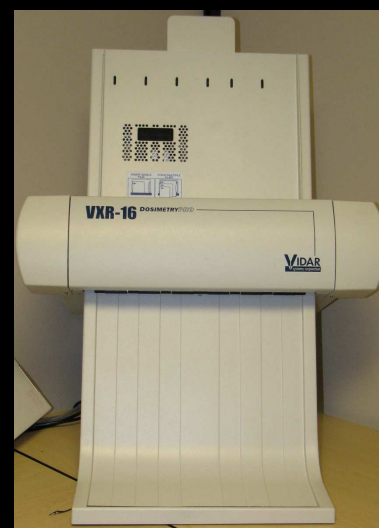
RANDO Phantoms

- Phantom was imaged using tomotherapy's MVCT system
- Phantom was automatically repositioned in the vertical, longitudinal, and lateral directions
- Roll corrections made by adjusting treatment start angle
- Yaw and pitch corrections applied manually by moving and re-imaging phantom



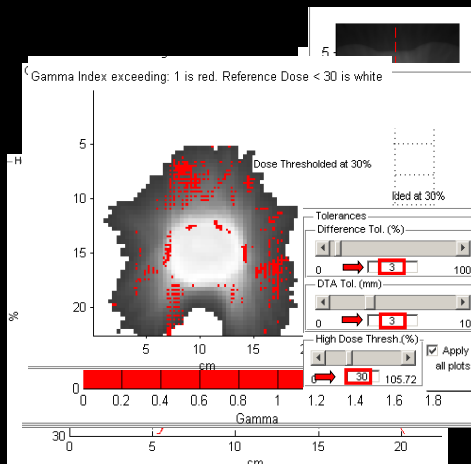
RANDO Phantoms

- EDR2 films were processed at least one hour after exposure in batches of five films
- Films were scanned using a Vidar 16 Dosimetry Pro and analyzed using Tomotherapy QA software and RIT dosimetry software
- Calculated and measured dose distributions were registered using fiducial-based registration system (*marks placed on the film prior to irradiation*)



RANDO Phantoms

- Horizontal profiles, vertical profiles, Gamma histograms, and Gamma pass/fail analysis were calculated for each test case
- Gamma calculation threshold parameters were set to 3% dose difference and 3-mm distance-to-agreement
- Analysis region of interest defined as area of film receiving over 30% of the prescribed dose



$$\Gamma(\vec{r}_e, \vec{r}_r) = \sqrt{\frac{|\vec{r}_e - \vec{r}_r|^2}{\Delta d^2} + \frac{[D_e(\vec{r}_e) - D_r(\vec{r}_r)]^2}{\Delta D^2}}$$

RANDO Phantoms

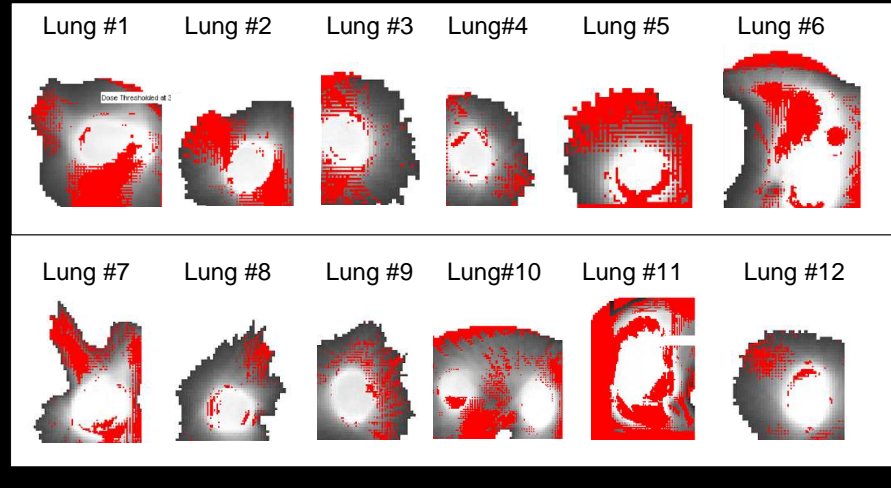
- Calculated and measured doses for the prostate test cases had better agreement than lung cases
- On average, the lung patients had 27.2% of pixels exceeding gamma and prostate patients had 14.7% of pixels exceeding gamma
- Only two prostate cases had greater than 20% of the pixels exceed gamma threshold
- In contrast, four lung test cases were below 20% pixel threshold

Lung Test Cases		
Patient Number	Mean Gamma Index	Percent Exceeding Gamma
1	0.82	30%
2	0.79	31%
3	0.71	23%
4	0.63	13% ↗
5	1.13	49%
6	0.87	29%
7	0.82	30%
8	0.55	10% ↗
9	0.64	16% ↗
10	0.77	27%
11	4.57	55% ↗
12	0.59	12% ↗

Prostate Test Cases		
Patient Number	Mean Gamma Index	Percent Exceeding Gamma
1	0.55	6%
2	0.61	18%
3	0.62	14%
4	0.67	18%
5	0.65	19%
6	0.69	20%
7	0.55	9%
8	0.72	24% ↗
9	0.57	8%
10	0.55	10%
11	0.74	23% ↗
12	0.50	5%

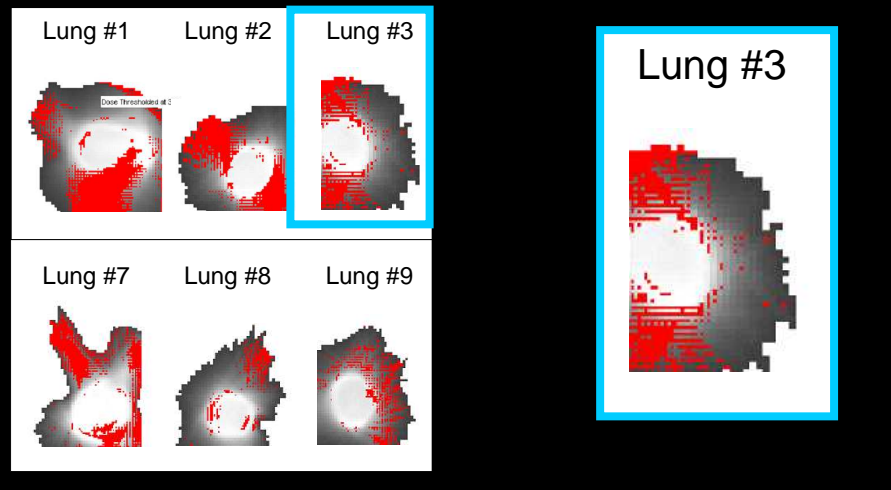
RANDO - Results

- Greatest discrepancy between calculated and measured occurs at/near drastic change in tissue density



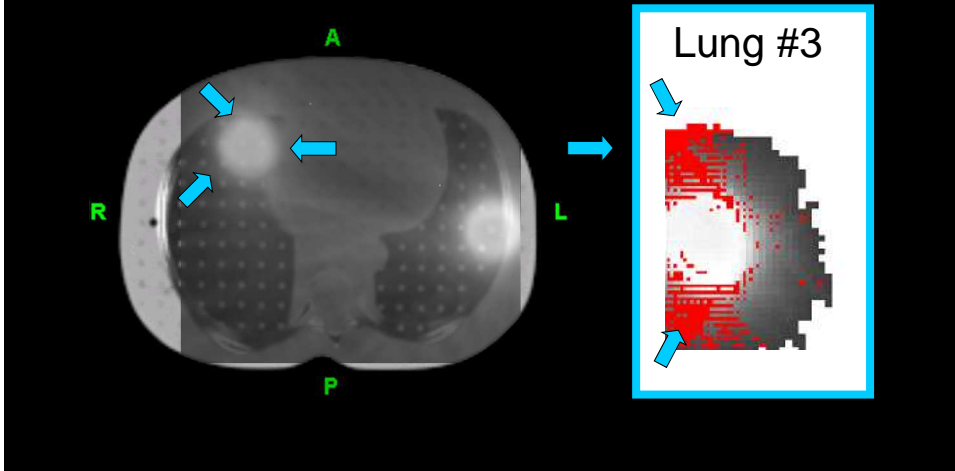
RANDO - Results

- Greatest discrepancy between calculated and measured occurs at/near drastic change in tissue density



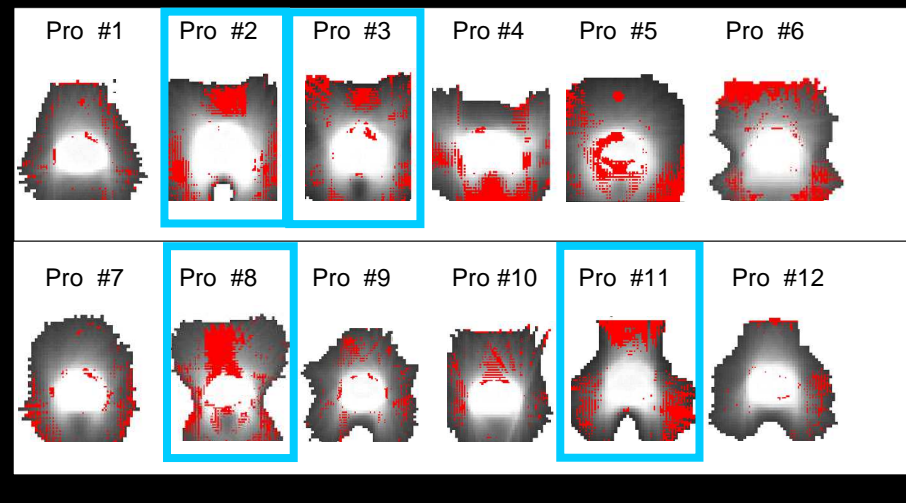
RANDO - Results

- Greatest discrepancy between calculated and measured occurs at/near drastic change in tissue density



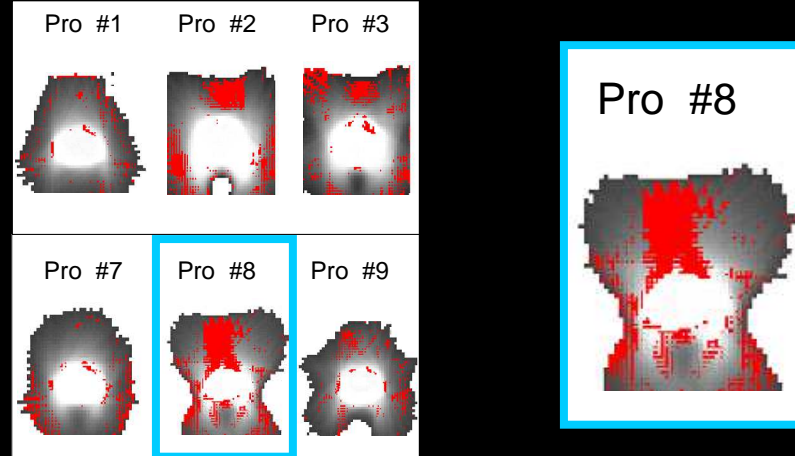
RANDO - Results

- Prostate cases 2, 3, 8, & 11 had greatest discrepancy between calculated and measured located at pubic symphysis



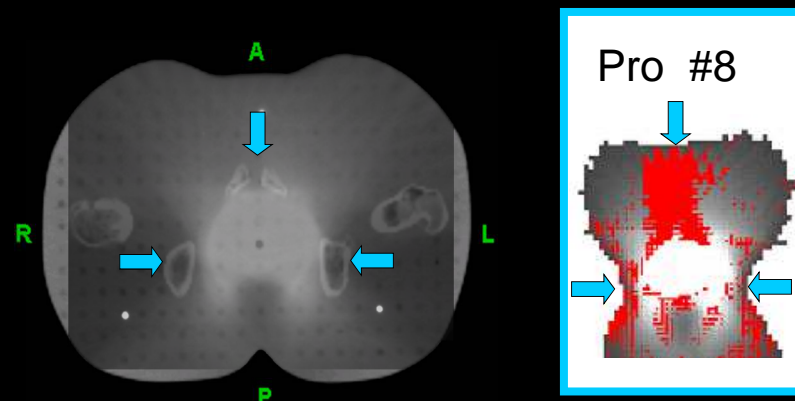
RANDO - Results

- Prostate cases 2, 3, 8, & 11 had greatest discrepancy between calculated and measured located at pubic symphysis



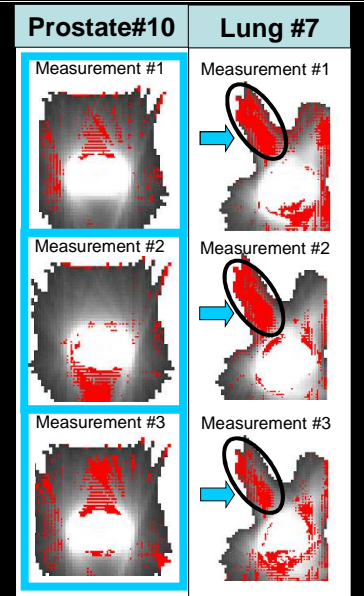
RANO - Results

- Prostate cases 2, 3, 8, & 11 had greatest discrepancy between calculated and measured located at pubic symphysis



RANDO - Results

- Reproducibility of film dosimetry was tested for a prostate and a lung case with repeat measurements occurring on three separate occasions
- Standard deviation for number of pixels exceeding the gamma threshold was 3.9%
- Prostate cases were not consistent in spatial location of dose errors between measurements
- Spatial location of the maximum error for the lung cases was consistent



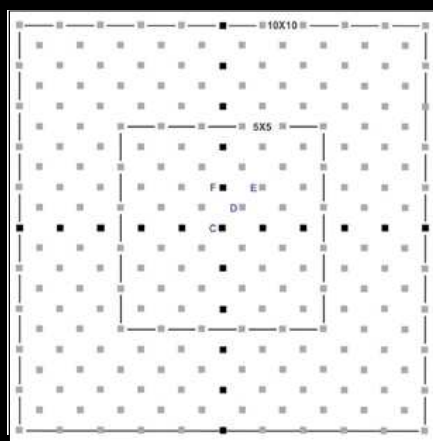
Array Detectors for Patient Specific QA

Array Detectors

- Array detectors are a new class of measurement device that utilize grid of detectors to absorbed dose across a 2D plane
- These devices have become popular because they can be used to provide a large number of dose measurements with the results available immediately
- Furthermore, with proper calibration, they can provide absolute dose verification
- However, the existing array detectors have low spatial resolution which limits their role to routine QA of a pre-commissioned IMRT technique



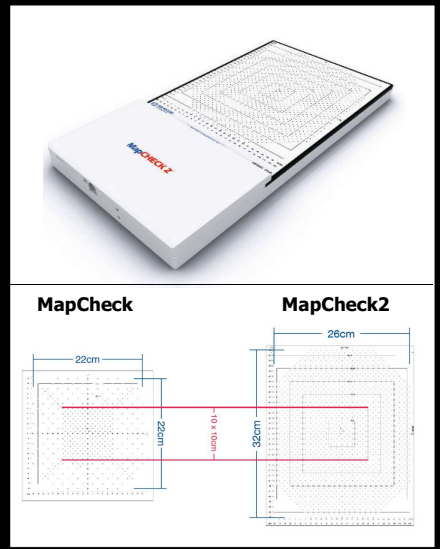
MapCheck: Overview



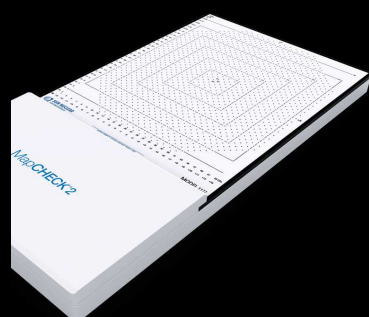
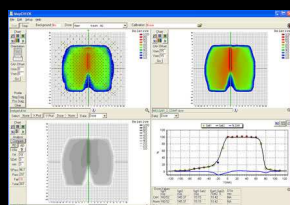
- The first commercially available array device was the MapCHECK
- The original MapCHECK consisted of 445 N-Type diodes that are in a 22 x 22 cm² array
- Each detector has an active area of 0.8 x 0.8-mm
- The Outer Band Array has 14.04-mm horizontal and vertical spacing
- The Inner 10 x 10-cm Array has 7.07-mm horizontal and vertical spacing

MapCheck: Overview

- The new MapCHECK2 has improved resolution over the original device
- It consists of 1527 N-Type diodes that are in a $22 \times 22 \text{ cm}^2$ array
- Each detector has an active area of $0.8 \times 0.8\text{-mm}$
- The array has 7.07-mm uniform spacing throughout array
- The MapCHECK2 also has a larger area than the original device

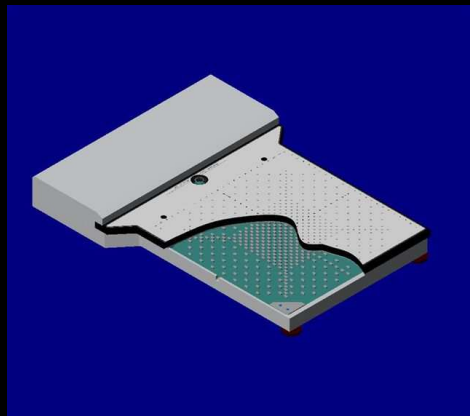


MapCheck: Overview



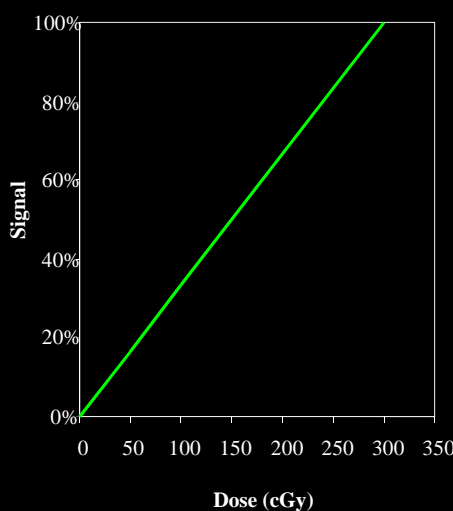
- The MapCHECK and MapCHECK 2 are two of the most widely used IMRT QA devices
- Advantages of these devices include:
 - Small Diode Size ($0.8 \text{ mm} \times 0.8 \text{ mm}$)
 - Linear Response
 - Reproducibility
 - Convenience of Setup
 - Real-Time Analysis
- Disadvantages include:
 - Energy Dependence
 - Differential Response to Scattered Radiation
 - Angular Dependence of Dose Sensitivity

MapCheck: Overview



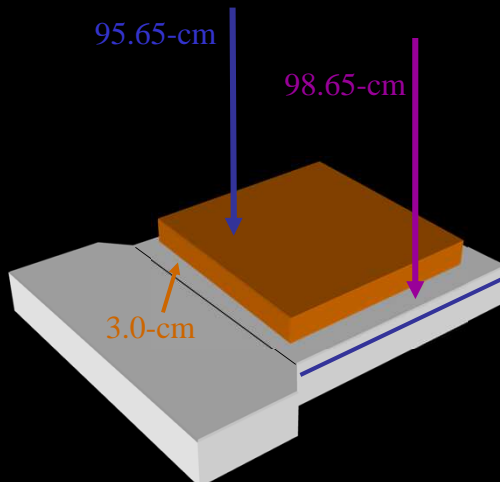
- The N-Diodes used in the MapCHECK arrays are a proprietary design that makes them very resistant to radiation damage (*compared to other N-Type Diodes*)
- The MapCHECK diodes are soldered to metal pads on two large circuit boards, and the two circuit boards are mounted parallel to one another with an air gap between them

MapCheck: Dose and Temp Response



- The response of the system is linear with dose
- The relative calibration is highly stable and publications indicate that it is stable for 6 months
- However, the N-Type diodes do have a temperature coefficient of 0.54% / °C
- As such it is recommended that the MapCHECK arrays be stored at a temperature close to that of the treatment room

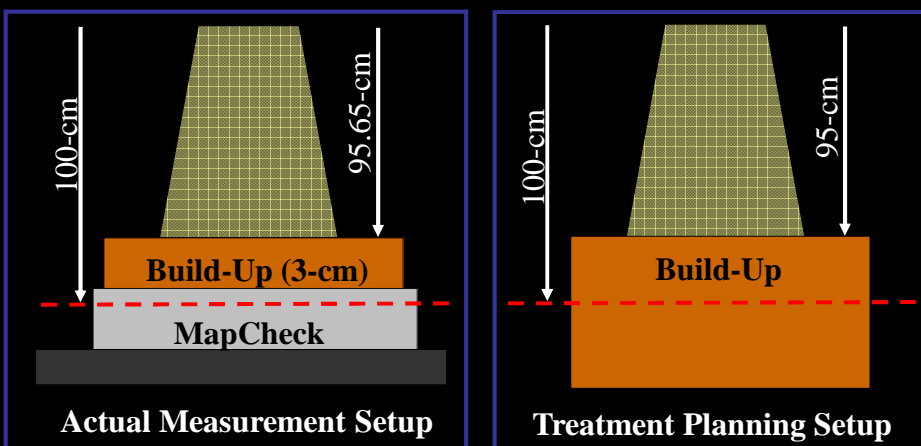
MapCheck: Planar Dosimetry Setup



- The system has a radiological buildup of 2 g/cm^2 to the detector junctions
- The physical thickness of the buildup is 1.35-cm
- The system also has 2.7 g/cm^2 of Backscatter
- As such, the system can be used with or without addition water-equivalent build-up material

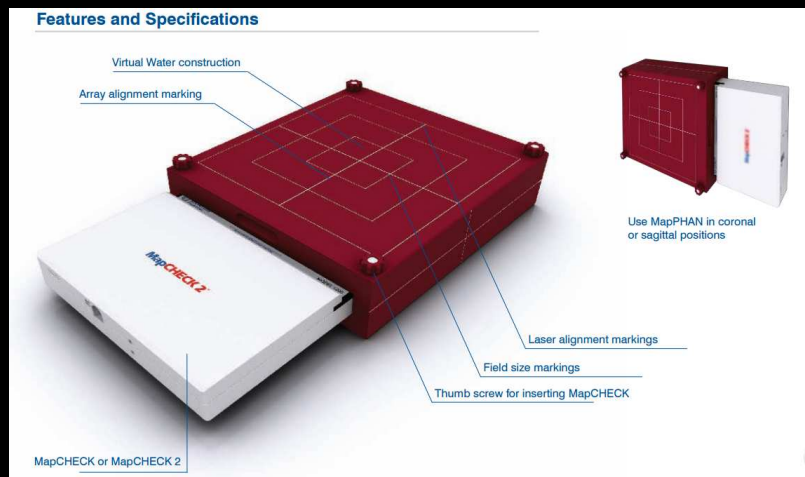
Jursinic et al. Med Phys 30:870

MapCheck: Planar Dosimetry Setup

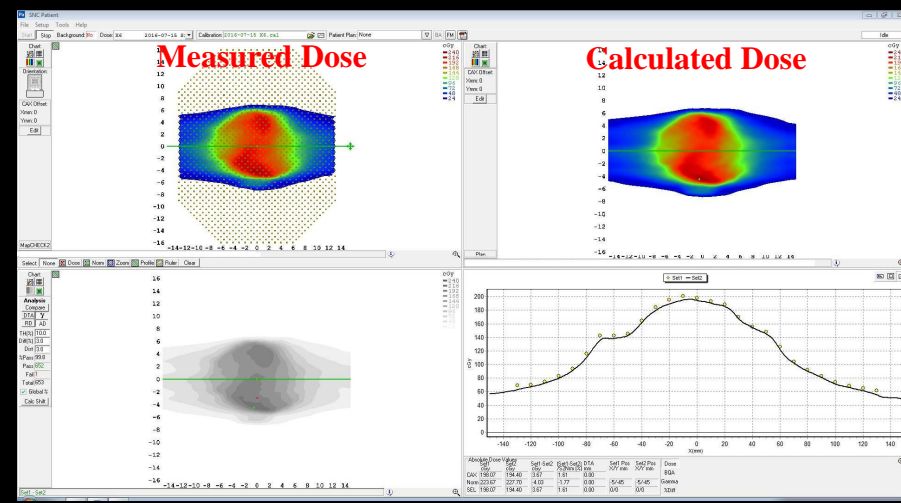


Jursinic et al. Med Phys 30:870

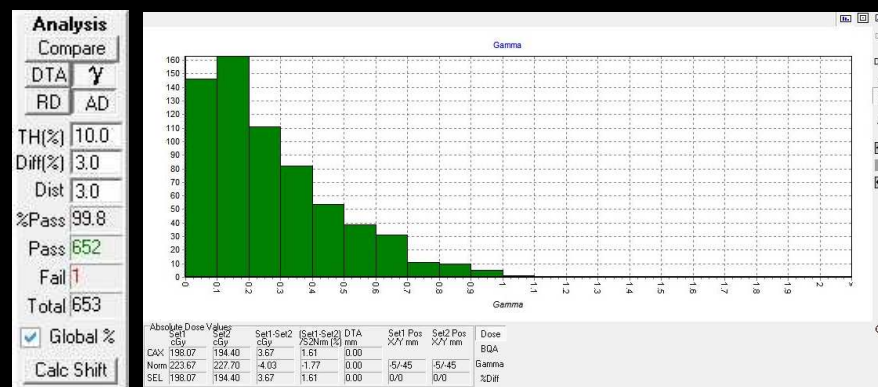
MapCheck: MapPHAN



MapCheck: Software Analysis

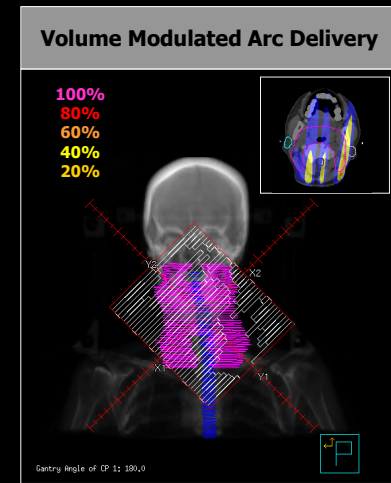


MapCheck: Software Analysis

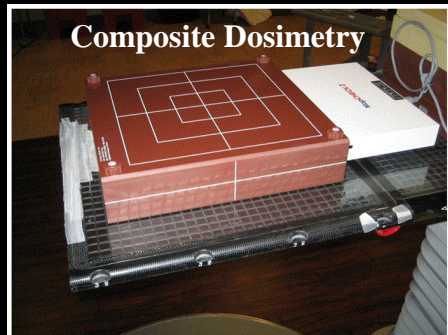


MapCheck: Rotational Delivery

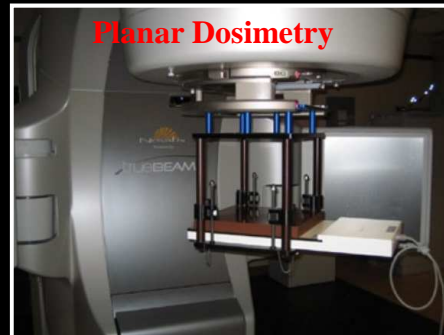
- The MapCheck arrays were designed for performing field-by-field planar dosimetry
- Nelms et al. conducted a survey of 64 MapCheck users in 2006 to determine their IMRT QA practices
 - 64.1% said that they use field-by-field analysis 100% of the time
 - 32.8% said that they use the single-gantry-angle composite technique for more than 75% of all IMRT plans
- More recently, an increasing number of MapCheck users are interested in performing composite dosimetry for rotational delivery techniques



MapCheck: Rotational Delivery



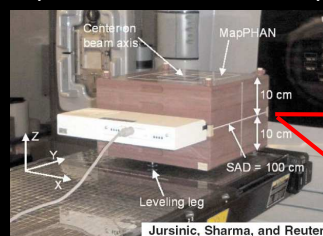
Keeling et al. J. Clin Med Phys 14 (6) 2013



Jin et al. J. Clin Med Phys 15 (3) 2014

MapCheck: CT Artifacts

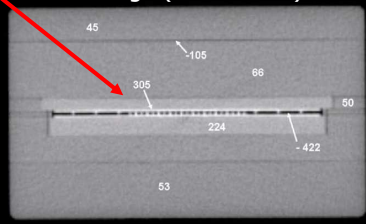
MapPHAN Measurement Setup



KVCT Image with Artifacts



MVCT Image (No Artifacts)

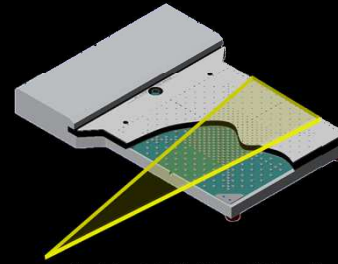
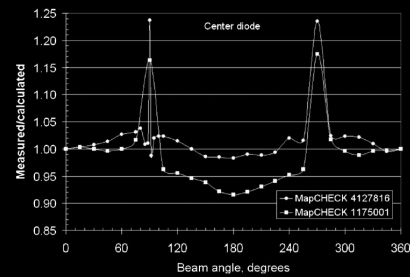


- KVCT images will show streak artifacts from the high atomic number materials on the circuit boards
- Heterogeneous dose calculations will result in distorted dose distributions

Jursinic et al. Med Phys 37, June 2010

MapCheck: Angular Dependence

- Using array devices for rotational delivery presents additional challenges
- Jursinic et al. reported that the angular dependence of a conventional MapCHECK was as great as 20%
 - *The MapCHECK has an over-response of 24% at 90° and 270°*
 - *The MapCHECK has an under-response of 8% at 180°*
- This angular response is believed to be due to multiple design properties of the MapCHECK



Jursinic et al. Med Phys 37, June 2010

MapCheck: Angular Dependence

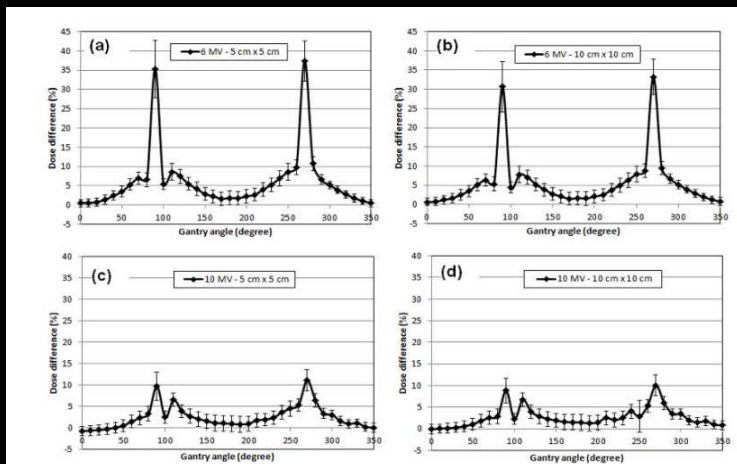
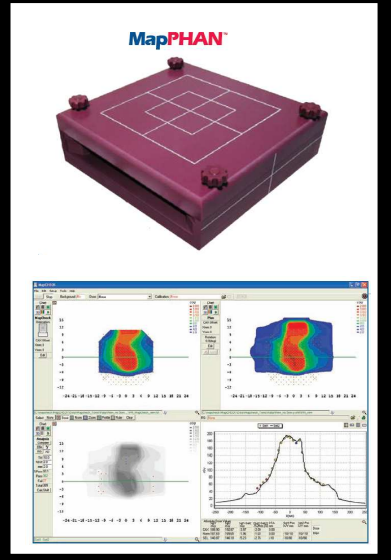


FIG. 4. The percent dose difference between measurement using MapCHECK 2 and planning (all measurement and planning points within a $2 \text{ cm} \times 2 \text{ cm}$ area were averaged and compared) at different gantry angles for different energies (6 MV and 10 MV) and field sizes ($5 \text{ cm} \times 5 \text{ cm}$ and $10 \text{ cm} \times 10 \text{ cm}$).

Keeling et al. J. Clin Med Phys 14 (6) 2013

MapCheck: Angular Dependence

- There are several published techniques for addressing angular dependence
 1. Ignore the angular dependence and accept a high pass/fail threshold
 2. Use a custom phantom to correct for the intrinsic asymmetry of the diodes
 3. Change the design by filling the air gap with sheets of Lucite with custom-machined slots for the diodes and by adding pieces of copper to offset the intrinsic asymmetry of the diodes
 4. Computationally correct the raw measured data for each gantry angle during data
 5. Computationally adjust the calculated doses from the planning system based on the gantry angle



MapCheck: QA Study #1

- Keeling *et al.* generated IMRT treatment plans using Eclipse for 10 H&N and 10 Prostate patients
 - Two beam energies (6 and 10 MV)
 - 5.0 cm of water-equivalent buildup above and below the detector plane (MapPHAN)
 - Raw CT scan was used without any post-processing or correction for asymmetric diode sensitivity
 - Calibrated by a standard protocol using a 10 × 10 cm² field instructed by the vendor
 - Step-and-Shoot results were measured for patient gantry angle composite (PGAC), single gantry angle composite (SGAC), and field by field (FBF)

Head and Neck			
Patient No.	No. of Beams	Total MUs	No. of Segments
1	12	1087	192
2	12	879	140
3	9	583	130
4	9	1039	113
5	7	420	107
6	18	1077	244
7	12	808	188
8	12	877	162
9	14	810	159
10	10	775	188

Prostate			
No. of Beams	Total MUs	No. of Segments	Energy
7	494	107	10 MV
9	472	133	10 MV
9	317	122	10 MV
9	550	149	6 MV
9	366	133	10 MV
9	438	128	6 MV
7	572	108	6 MV
7	387	98	6 MV
8	433	117	6 MV
7	363	96	6 MV

Keeling et al. J. Clin Med Phys 14 (6) 2013

MapCheck: QA Study #1

TABLE 2. Average passing rates of the γ test for the different IMRT QA techniques with different criteria.

Dose Diff-DTA Criteria	QA Method	Head and Neck		Prostate	
		Mean	SD	Mean	SD
C1 (1%-1 mm)	PGAC	56.1	8.6	58.7	8.5
	SGAC	70.9	8.3	68.3	8.1
	FBF	71.1	6.6	66.5	7.2
C2 (2%-2 mm)	PGAC	90.7	4.8	91.0	3.7
	SGAC	94.7	3.0	97.9	3.5
	FBF	95.0	1.9	97.2	1.9
C3 (3%-3 mm)	PGAC	98.8	1.1	98.9	0.6
	SGAC	99.6	0.4	100.0	0.0
	FBF	99.5	0.3	100.0	0.1

Keeling et al. J. Clin Med Phys 14 (6) 2013

MapCheck: QA Study #1

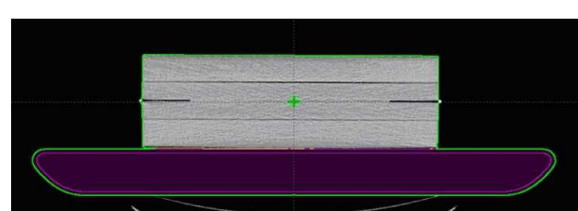


FIG. 2. Modeling of the Varian couch top with 10 cm height of solid water blocks with isocenter placed at 5 cm depth in the Eclipse treatment planning system.

TABLE 5. Average dose difference of ionization chamber measurements for three different situations concerning the couch.

	S1 (P-WC vs. M-WC)	S2 (P-WOC vs. M-WC)	S3 (P-WOC vs. M-WOC)
H&N	1.0%±0.7%	-0.4%±0.9%	0.4%±1.7%
Prostate	1.7%±1.1%	0.0%±1.0%	0.1%±1.5%
Overall	1.3%±1.0%	-0.2%±1.0%	0.3%±1.5%

Keeling et al. J. Clin Med Phys 14 (6) 2013

MapCheck: QA Study #2

- Jin *et al.* generated RapidArc treatment plans using Eclipse for 14 patients selected from different treatment sites
 - Four beam energies (6, 8, 10, and 15 MV)
 - 5.0 cm of water-equivalent buildup above and below the detector plane
 - Dose was computed using anisotropic analytical algorithm (AAA) with a calculation grid of 2 mm
 - Raw CT scan was used without any postprocessing or correction for asymmetric diode sensitivity
 - Calibrated by a standard protocol using a $10 \times 10 \text{ cm}^2$ field instructed by the vendor

TABLE 1. Summary of the RapidArc QA patients.

Patient Number	Treatment Site	No. of Arcs
1	Brain	2
2	Brain	1
3	Chest	1
4	Head and Neck	1
5	Head and Neck	2
6	Head and Neck	1
7	Lung	1
8	Lung	2
9	Pancreas	1
10	Prostate	1
11	Prostate	1
12	Rectum	1
13	Stomach	1
14	Stomach	1

Jin et al. J. Clin Med Phys 15 (3) 2014

MapCheck: QA Study #2

TABLE 2. Mean passing rates (%) of the γ test for the RapidArc QA techniques with $10 \times 10 \text{ cm}^2$ field MapCHECK 2 calibration.

		MapPHAN QA			IMF QA			IMF _{ACTUAL} QA		
		1%/1 mm	2%/2 mm	3%/3 mm	1%/1 mm	2%/2 mm	3%/3 mm	1%/1 mm	2%/2 mm	3%/3 mm
6 MV	Mean	55.8	84.6	94.4	60.2	91.0	97.8	57.1	90.4	98.0
	S.D.	18.1	14.9	7.5	8.1	5.4	2.4	8.7	6.1	2.5
8 MV	Mean	77.2	96.7	99.3	56.9	89.8	97.7	57.4	90.8	97.9
	S.D.	12.5	3.6	1.1	7.0	5.4	2.4	7.9	5.6	2.0
10 MV	Mean	74.8	95.0	98.8	62.2	92.6	98.2	59.2	91.8	98.4
	S.D.	14.2	7.4	2.4	7.8	4.1	1.9	9.4	5.8	2.0
15 MV	Mean	81.4	97.9	99.6	58.7	90.1	98.0	58.0	91.3	98.1
	S.D.	11.2	1.7	0.5	7.9	5.4	2.1	8.1	4.8	2.1

S.D. = standard deviation.

Composite

Planar

Jin et al. J. Clin Med Phys 15 (3) 2014

MapCheck: QA Study #2

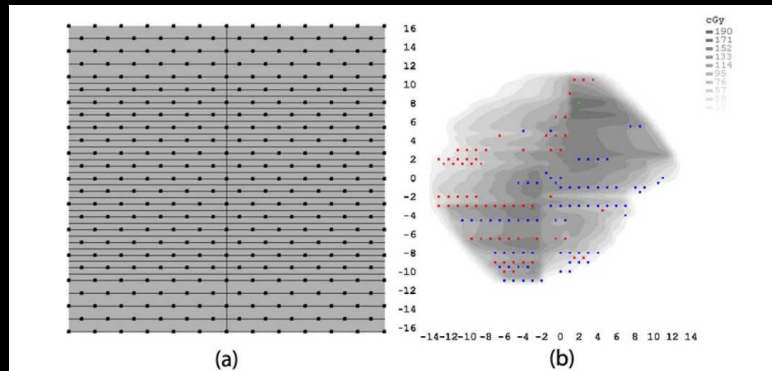


FIG. 6. The tongue-and-groove effect on the IMF QA demonstrated by continuous hot or cold spots along MLC trajectory: (a) MapCHECK 2 diode points overlaid on the HD-MLC pattern (inner leaf width = 2.5 mm, outer leaf width = 5 mm, and diode size = $0.8 \times 0.8 \text{ mm}^2$), and (b) failed points of 15 MV IMF QA using $2\% / 2 \text{ mm}$ criteria for Patient #3. (Red = measurement is high; blue = calculation is high.)

Common errors in planar dosimetry (IMF Mount)

Jin et al. J. Clin Med Phys 15 (3) 2014

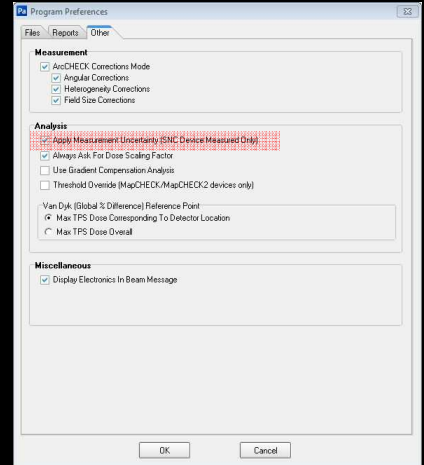
MapCheck: QA Study #3

- Bailey *et al.* evaluate 109 static gantry IMRT fields and 40 VMAT Arcs from different treatment sites
 - Measurements performed in a planar setup
 - 5.0 cm of water-equivalent buildup above and below the detector plane (MapPHAN)
 - Dose was computed using anisotropic analytical algorithm (AAA)
 - A water-equivalent phantom with source-to-detector distance of 100 cm and water-equivalent depth of 5 cm (CT not used)
 - Analyzed using MapCheck software in absolute mode, global % difference normalization to the max planned dose, and a 10% threshold
- 5 static-gantry IMRT plans for head/neck (*49 fields*)
- 9 static-gantry IMRT plans for prostate (*60 fields*)
- 10 RapidArc plans for head/neck (*20 arcs*)
- 10 RapidArc plans for prostate (*20 arcs*)
- Each field or arc was delivered on a Varian Trilogy linear accelerator system

Bailey et al. J. Clin Med Phys 17 (2) 2016

MapCheck: QA Study #3

- Sun Nuclear Measurement Uncertainty function applies certain corrections to the analysis
 - Array calibration correction (*approximated from a study dealing with the original MapCHECK device*)
 - A correction for assumed accelerator output and room temperature differences between the time of array calibration and actual measurement
 - A correction for an assumed error in setup source-to-surface distance (SSD)
- Bailey *et al.* measured the impact of applying this correction



Bailey et al. J. Clin Med Phys 17 (2) 2016

MapCheck: QA Study #3

Statistics	3%/3 mm MCU _{on}	3%/3 mm MCU _{off}	3%/3 mm (on - off)	%Diff _{eff} for 3%/3 mm
Prostate	average minimum maximum SD	97.2 89.8 100.0 2.8	95.5 83.8 100.0 4.1	1.7 0.0 7.8 1.8
H&N	average minimum maximum SD	97.4 92.6 100.0 1.7	96.3 90.3 99.7 2.3	1.0 0.0 4.0 1.0

SD = standard deviation

Statistics	2%/2 mm MCU _{on}	2%/2 mm MCU _{off}	2%/2 mm (on - off)	%Diff _{eff} for 2%/2 mm
Prostate	average minimum maximum SD	87.1 69.9 99.4 8.5	81.6 60.7 96.8 10.1	5.5 0.7 11.8 2.7
H&N	average minimum maximum SD	91.3 83.0 97.4 3.1	87.8 77.7 95.1 4.0	3.5 1.2 8.3 1.7

SD = standard deviation

Bailey et al. J. Clin Med Phys 17 (2) 2016

MapCheck: QA Study #3

TABLE 5. MapCHECK Uncertainty results for VMAT with DTA 3%/3 mm.

Statistics	3%/3 mm MCU _{on}	3%/3 mm MCU _{off}	3%/3 mm (on - off)	%Diff _{off} for 3%/3 mm
Prostate	average	96.2	92.8	3.4
	minimum	92.7	87.3	1.6
	maximum	98.7	96.5	5.5
	SD	2.0	2.7	1.1
H&N	average	95.8	92.2	3.5
	minimum	90.4	86.2	1.3
	maximum	99.5	97.7	8.7
	SD	2.4	3.4	1.7

SD = standard deviation

TABLE 8. MapCHECK Uncertainty results for VMAT with gamma 2%/2 mm.

Statistics	2%/2 mm MCU _{on}	2%/2 mm MCU _{off}	2%/2 mm (on - off)	%Diff _{off} for 2%/2 mm
Prostate	average	90.6	85.2	5.3
	minimum	83.8	77.9	2.8
	maximum	95.2	91.8	9.3
	SD	3.5	4.3	1.5
H&N	average	90.2	84.5	5.8
	minimum	83.1	73.4	2.6
	maximum	96.4	93.8	10.3
	SD	4.2	5.5	1.9

SD = standard deviation

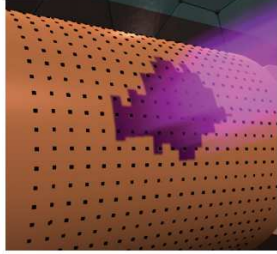
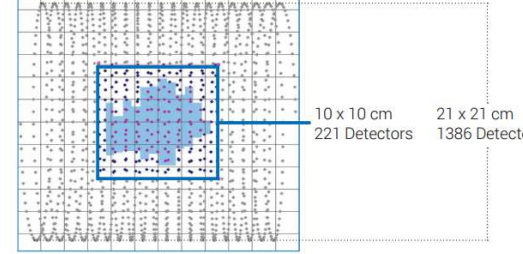
Bailey et al. J. Clin Med Phys 17 (2) 2016

ArcCheck

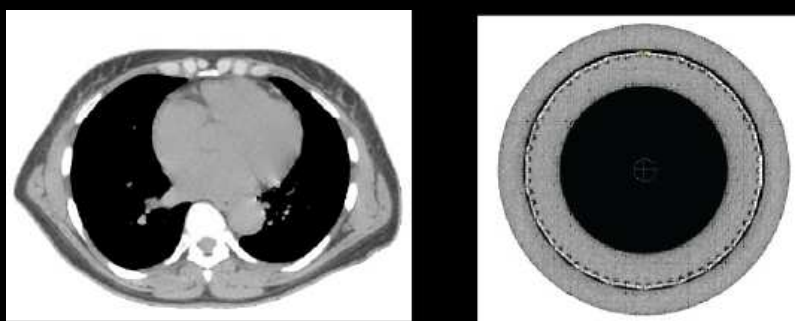
- Sun Nuclear ArcCHECK is a true 4D array specifically designed for VMAT
 - QA 1,386 SunPoint Diode Detectors (0.019 mm^3)
 - Consistent Beams Eye View (BEV) for all gantry angles measuring entrance and exit dose
 - Real-time electrometer measures every pulse, as well as composite and sub-arcs
 - ArcCHECK detectors are always facing the delivery beam regardless of gantry angle. The detector geometry relative to the BEV remains constant



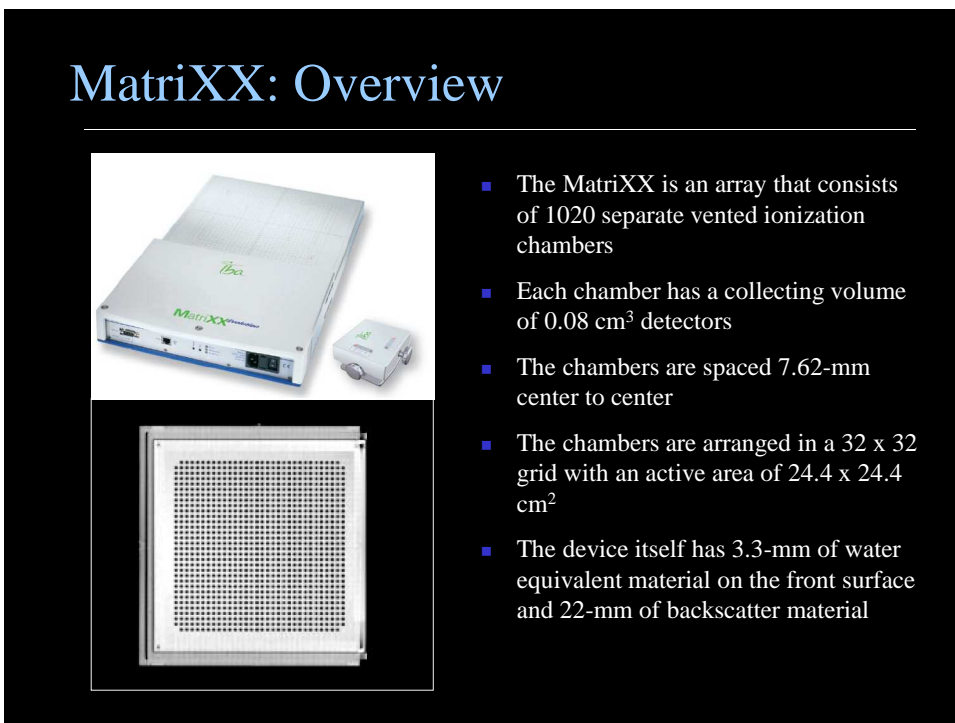
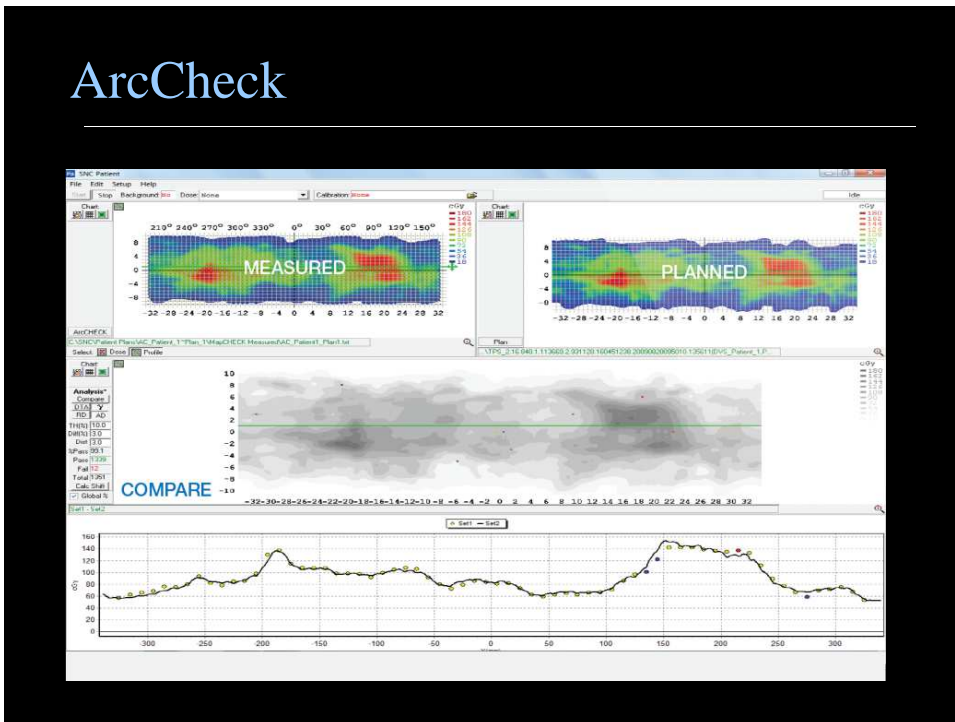
ArcCheck

Beam Delivery 	ArcCHECK Detector BEV  <p>10 x 10 cm 21 x 21 cm 221 Detectors 1386 Detectors</p>
<ul style="list-style-type: none"> ▪ Detectors are arranged on a helical grid which increases the sampling rate and reduces BEV detector overlap and shadowing ▪ An ArcCHECK 10 x 10 cm² area contains 221 detectors; equivalent to the detector density in a MapCHECK 2 ▪ Entrance and exit dose are measured, effectively doubling the detector density in the measurement field 	

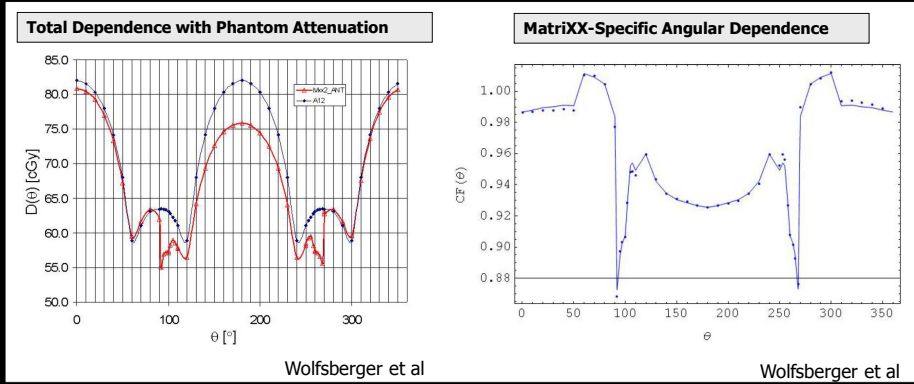
ArcCheck



- Place detectors in best geometry possible to measure rotational beam
- Forces TPS to account for topography and heterogeneities
- Phantoms are ideally shaped like a patient
- Solid inserts are available to provide homogeneous density



MatriXX: Angular Dependence



- The total effect due to the inherent angular dependency and the attenuation due to rectangular phantom used in the QA setup
- Angular dependency of other MatriXX arrays has reported to be similar in shape but slightly different in magnitude

MatriXX: Angular Dependence

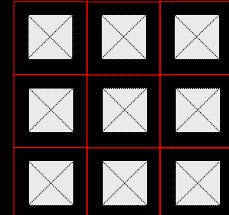
- There are several techniques for addressing angular dependence
 - Ignore the angular dependence and accept a high pass/fail threshold
 - Use a custom phantom to correct for the angular dependence
 - Computationally correct the raw measured data for each gantry angle during data
 - Computationally adjust the calculated doses from the planning system based on the gantry angle



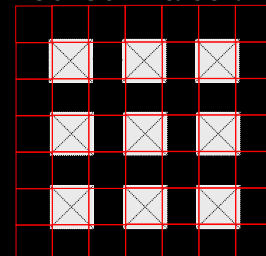
MatriXX: Volume Averaging

- The finite size of the ion-chamber array results in a measurable volume-averaging effect
- The FWHM for each chamber is about 5.8 mm assuming a Gaussian response function
- This volume-averaging effect should be properly taken into account when comparing measured and calculated doses
- Ideally, the calculated doses should be also be volume averaged to a 3.8 x 3.8-mm array that is centered over each of the ionization chambers

7.6 x 7.6 mm Calc Grid



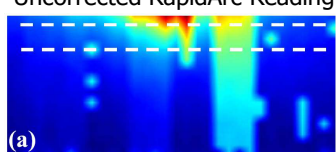
3.8 x 3.8 mm Calc Grid



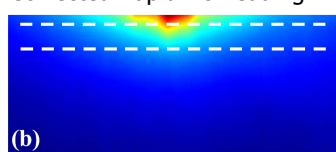
MatriXX: Blank Image Bias

- A positive bias accumulates during MatriXX measurements in the movie mode (*used for IMRT QA*)
- Its contribution to dose error in the high dose regions is limited, but it can cause appreciable dose errors in peripheral regions
- Han et al. measured this effect and suggested that the background compensation (which is performed for each individual frame) as one cause
- They suggested selecting a sample time greater than 2 seconds in order to reduce the bias accumulation for IMRT QA
- For rotational delivery, a correction must be applied to the raw readings

Uncorrected RapidArc Reading



Corrected RapidArc Reading

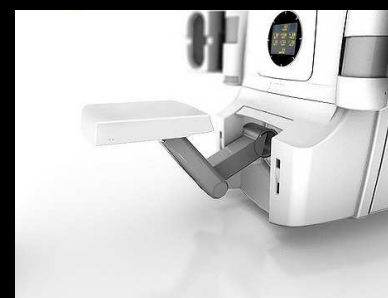


Han et al. Medical Physics, Vol. 37, No. 7, July 2010

EPID and Logfile Patient Specific IMRT QA

EPID Dosimetry and Log Files

- Linacs with EPID imagers have the capability to measure dose directly with the detector array
- In addition, linac have log files that store information about the treatment delivery
- This data can be used either separately, or together, in the patient IMRT QA process



EPID Imager



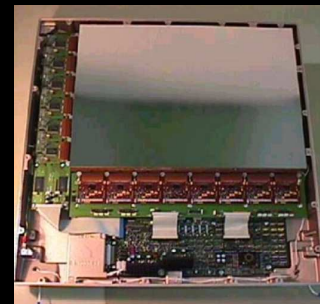
R-Arm

- Older Type of Support
- Positional accuracy of $\pm 5\text{mm}$
- No Motor Brakes

R-Arm

- Available since 2003
- Positional accuracy of $\pm 1\text{mm}$
- Motors with Brakes

EPID Imager



TrueBeam MV Arm

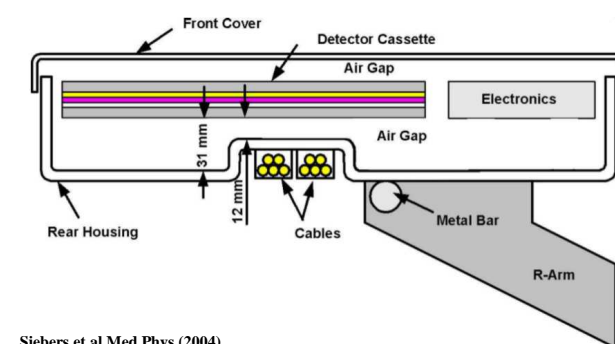
- Positional accuracy of $\pm 0.5\text{mm}$
- aSi 1000 Detector Panel

EPID Imager

Imager Type	Acquisition Unit	Max. Readout Speed	Matrix	Resolution
IDU 11 (40x30 cm ²)	IAS2 (aSi 500)	15fps	512 x 384	0.78mm
	IAS3 (aSi 500 II)	30fps	512 x 384	0.78mm
IDU 20 (40x30 cm ²)	IAS2 (aSi 500)	15fps	512 x 384	0.78mm
	IAS3 (aSi 500 II)	30fps	512 x 384	0.78mm
	IAS3 (aSi 1000)	30fps	1024 x 768	0.39mm

EPID Imager

Cross-sectional cut through an aSi EPID

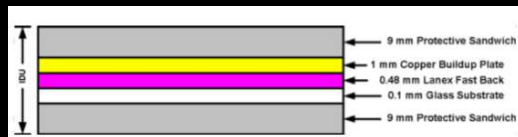


aSi EPIDs

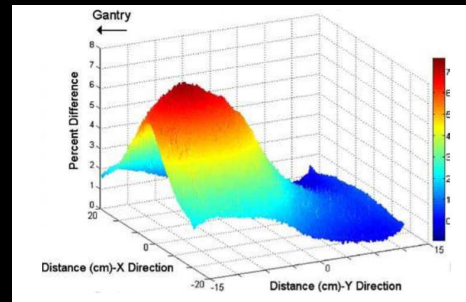
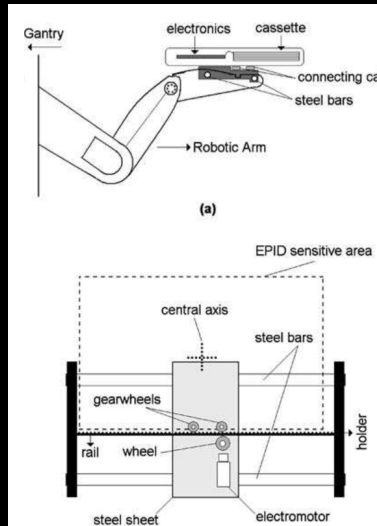
- Metal Plate
- Phosphor Scintillator
- Array of photodiodes
- 40cm x 30cm
- 1024 x 798 pixels
- 0.5-mm resolution

Corrections

- “Dark field”
- “Flood field”
(assumes uniform field, equalizes pixel-to-pixel gains)
- Bad pixel corrections



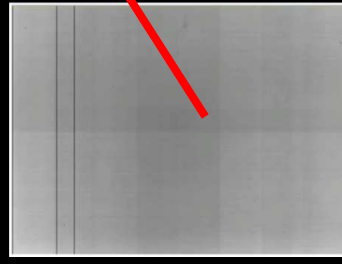
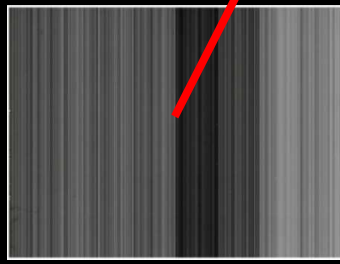
EPID Imager



Rowshanfarzad et al Med Phys (2010)

Portal Dosimetry

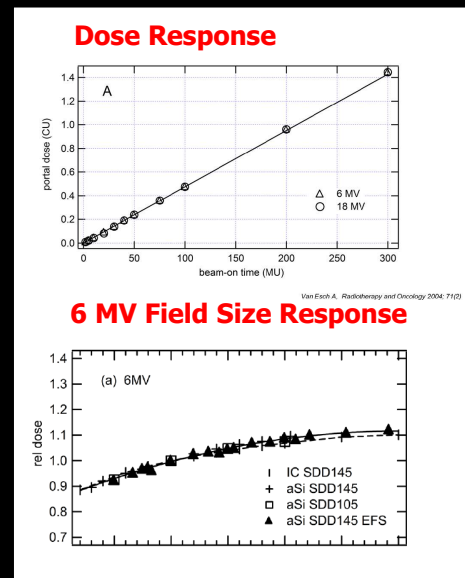
$$\left[\text{Object Image Beam On} - \text{Dark Field} \right] / \text{Flood Field} * k_{FF\text{mean}}$$



Flood Field Removes Beam and Scatter Asymmetry

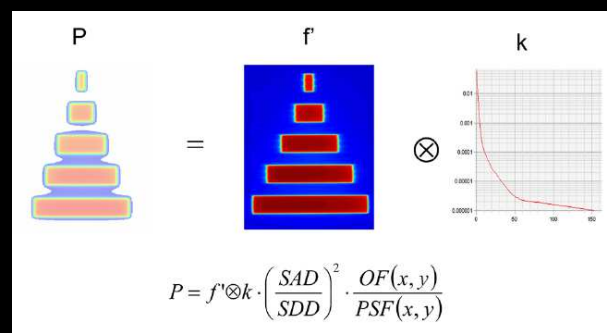
Portal Dosimetry

- In order to use a Varian EPID for portal dosimetry, it must first be calibrated
 - Field Size = 10x10 cm
 - SSD = 145 cm
 - Monitor Units = 100
- The reading is set to 1 “Calibrated Unit” (CU)
 - 1 CU is approximately 1 cGy
 - CU has a linear relationship with delivered dose



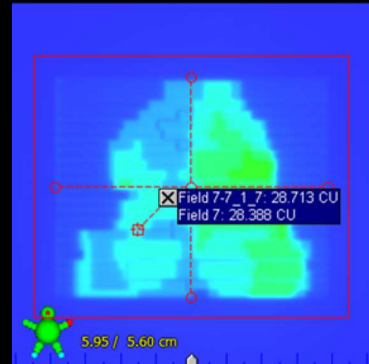
Portal Dosimetry

- Portal dosimetry prediction is calculated from a fluence map, not dose map
 - Part of the Varian Eclipse Planning System
 - Uses a dedicated algorithm



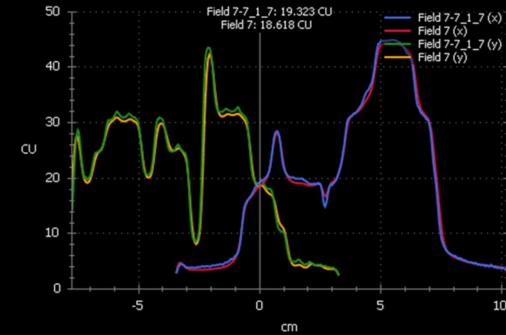
Portal Dosimetry

Blended: Field 7 - Field 7-7_1_7 - 0 deg



Point Dose Comparison

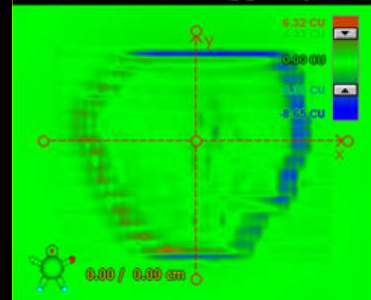
Profiles along Collimator Axes - Coll Rtn 0 deg



Profile Comparison

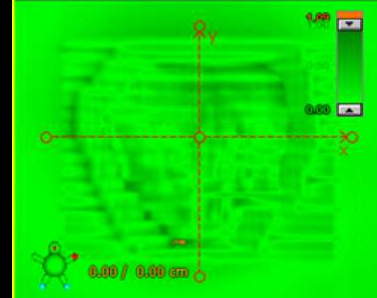
Portal Dosimetry

Dose Difference: Field 1 - Field 1-1_1_1 - 0 deg



Dose Difference

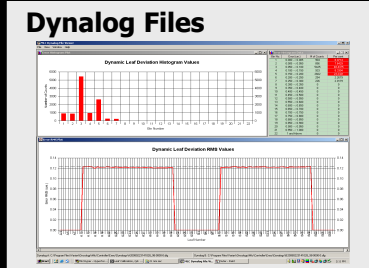
Gamma Evaluation: Field 1 - Field 1-1_1_1 - 0 deg



Gamma Analysis

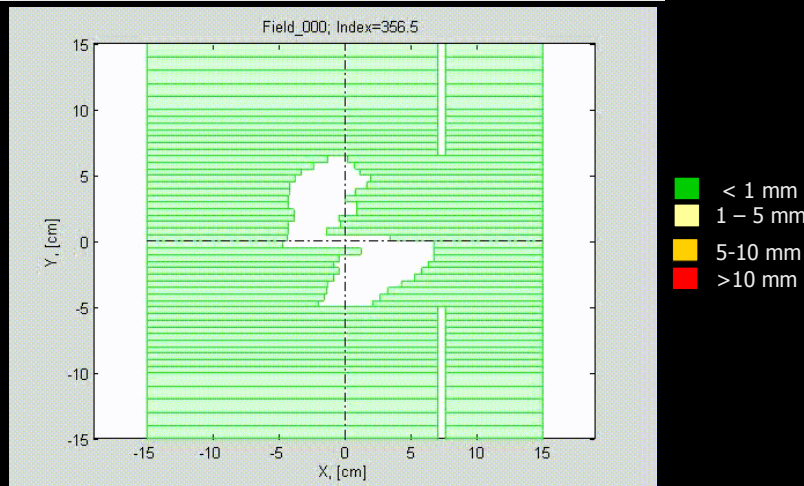
Dynalog and Trajectory Files

- The performance of Varian 120-leaf MLC's can be evaluated using the Dynalog files (*C-Series*) and Trajectory files (*TrueBeam*)
- The MLC controller records actual and expected MLC positions for each leaf
- Data is recorded every 50 msec and can be downloaded after treatment delivery
- Dynalog files can be viewed with the Varian Dynalog file viewer
- Trajectory logs require 3rd party software

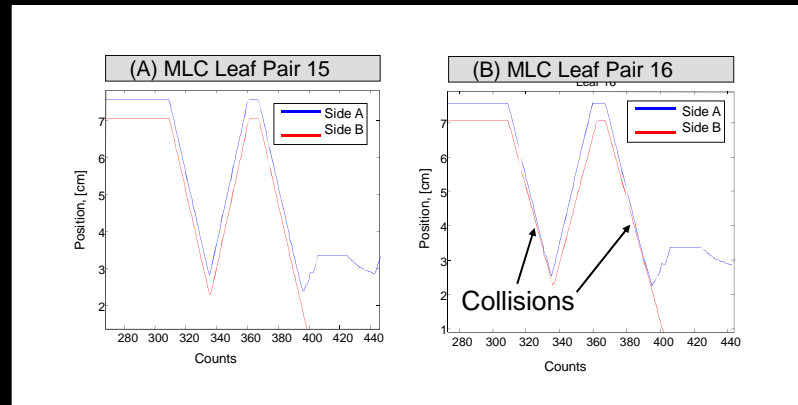


Dynalog and Trajectory Files

MLC Positional Error for a Prostate Case



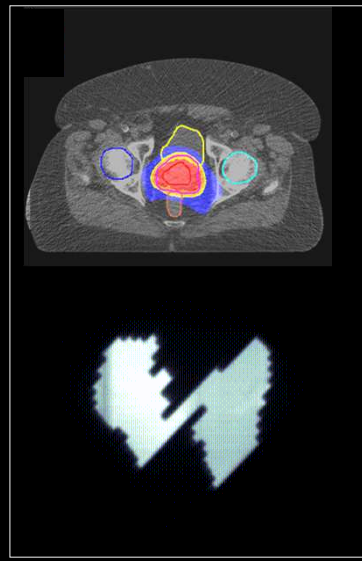
Dynalog and Trajectory Files



One potential problem during VMAT delivery is MLC collision from opposed MLC leafs due to degraded motor performance

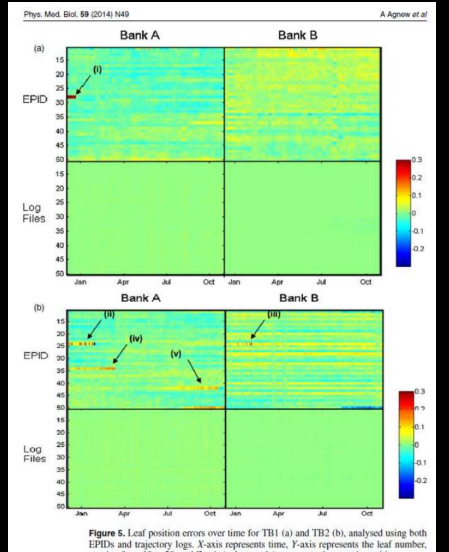
Dynamic EPID Imaging

- In addition to the Dynalog and Trajectory files, the position of the individual MLC leafs can be determined from CINE EPID imaging
- The position of the leaf tips can be extracted from the imaging data
 - *Pre-Treatment as part of IMRT QA*
 - *During actual patient treatment as daily IMRT QA*
- The spatial resolution is limited by the detector array size and position
- The temporal resolution is limited by the detector's frame capture rate



Dynamic EPID Imaging

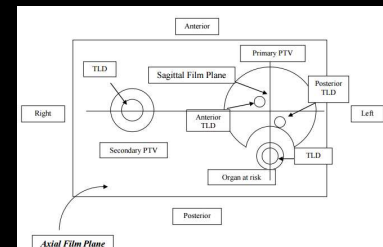
- The accuracy of the Dynalog and Trajectory files is unknown
 - *These files are a black box*
 - *No way to easily QA the logs*
 - *Does not take into consideration the actual dose*
- Agnew *et al.* compared log files and EPID data
- Found that errors were present in the EPID data, but not the log files



Error Detection in IMRT QA

Examples of failure to detect errors

- The 3%/3 mm gamma passing rate metric is commonly used for a range of dosimetric QA tasks
- 3%/3 mm gamma analysis passing rate may lack the sensitivity to detect many forms of systematic error
- In the most recent report from the Radiological Physics Center (RPC), only 82% of the institutions passed the end-to-end test with the anthropomorphic head and neck phantom
 - The H&N test has rather lenient dose difference and distance-to-agreement (DTA) criteria of 7% and 4 mm
 - Only 69% of the irradiations passed the narrowed TLD dose criterion of 5%



Examples of failure to detect errors

- Nelms *et al.* reported on variety of real-world cases where systematic errors were not detected by widely accepted methods for IMRT/VMAT dosimetric accuracy evaluation
 - 3%/3 mm gamma passing rates exceeded 99% for IMRT per-beam analyses
 - 3%/3 mm gamma passing rates ranged from 93.9% to 100% for composite plan dose analysis
- However, all cases had systematic errors that were detected only by using advanced diagnostic techniques and more sensitive metrics

Evaluating IMRT and VMAT dose accuracy: Practical examples of failure to detect systematic errors when applying a commonly used metric and action levels

Benjamin E. Nelms^{1,2}
Cora Lugo LLC, Milwaukee, Wisconsin 53261

Maria F. Chan³
Roxbury Regional Cancer Center, Basking Ridge, New Jersey 07920

Genevieve Jarry and Matthieu Lamothe⁴
Hôpital Maisonneuve-Rosemont, Montréal, QC H3T 2M4, Canada

John Lowden⁵
Indiana University Health - Golombok Hospital, Golombok, Indiana 46326

Carroll Hampton⁶
Levine Cancer Institute/Carolinas Medical Center, Concord, North Carolina 28025

Vladimir Ferghman⁷
Proton Therapy Institute, Naples, Florida 34102

(Received 24 April 2013; revised 25 September 2013; accepted for publication 4 October 2013; published 25 October 2013)

Purpose: This study (1) examines a variety of real-world cases where systematic errors were not detected by the commonly used metric and action levels for IMRT/VMAT dose accuracy evaluation, and (2) drills down to identify failure modes and their corresponding means for detection, diagnosis, and mitigation. The primary goal of detailing these case studies is to explore different, more sensitive methods to provide useful information about systematic errors in IMRT/VMAT delivery systems, and QA devices.

Methods: The authors present seven real-world case studies representing a variety of combinations of the treatment system (TPS), linear, delivery modality, and systematic error type. These case studies are typical to what might be used as part of an IMRT or VMAT commissioning test suite.

Results: This study is based on 119 composite plans for IMRT/VMAT dose accuracy evaluation, passing rates and action levels for composite plan dose analysis, and composite plan dose analysis.

Conclusion: Most of the relevant systematic errors can be understood when using only gamma

analysis for IMRT/VMAT commissioning. If alternative methods and metrics are used instead of (or in addition to) the conventional metrics, these errors are more likely to be detected, and only once they are detected can they be properly diagnosed and rooted out of the system. Requiring the use of more sensitive metrics will help the physician and manufacturer to have product validation by the manufacturers. For any systematic errors that cannot be removed, detecting and quantifying them is important as it will help the physician understand the limits of the system. The use of more sensitive metrics for IMRT/VMAT dose accuracy, IMRT/VMAT commissioning, along with product validation, would benefit from the refinement of the 3%/3 mm

Examples of failure to detect errors

TABLE I. Details of the case studies, including TPS, linac, energy, MLC type, delivery modality, and type of error.

ID	TPS	Linac/MV/MLC	Delivery modality	Error type
1	Pinnacle	Elekta 6 MV 80-leaf (10 mm)	IMRT (step and shoot)	TPS model setting
2	MSK	Varian 6 MV 120-leaf	IMRT (dynamic)	TPS model setting
3	Eclipse	Varian 15 MV 120-leaf	IMRT (dynamic)	TPS input data
4A	Monaco	Elekta 6 MV 80-leaf (4 mm)	IMRT (step and shoot)	TPS algorithm
4B	Monaco	Elekta 6 MV 80-leaf (4 mm)	VMAT (1 arc)	TPS algorithm
5	Pinnacle	Varian 6 MV 120-leaf	VMAT (2 arc)	TPS algorithm
6	Pinnacle	Elekta 10 MV 80-leaf	Open field	TPS phantom setting
7	Eclipse	Varian 6 MV 120-leaf	VMAT (2 arc)	TPS phantom setting

TABLE II. Passing rate method (per beam planar or composite), dosimeters, and analysis methods employed for each case study.

ID	Passing rate	Dosimeter(s)	Advanced diagnostic methods
1	Per-beam 2D	MapCHECK2	Dose profiles; 3D MGDR
2	Per-beam 2D	EPIDose	2%L/2 mm error pattern; 3D MGDR
3	Per-beam 2D	MapCHECK	2%L/2 mm error pattern; dose profiles; EPID-based
4A	Composite 3D	ArcCHECK	2%L/2 mm error pattern; dose profiles; 3D MGDR
4B	Composite 3D	ArcCHECK	2%L/2 mm error pattern; 3D MGDR
5	Composite 3D	Delta4; ArcCHECK	2%L/2 mm error patterns; dose profiles; 3D MGDR
6	Composite 3D	ArcCHECK	2%L/2 mm error pattern; ion chamber; 3D MGDR
7	Composite 3D	ArcCHECK	2%L/2 mm error pattern; 3D MGDR; dose grid inspection

Nelms et al. Med Phys 40 (11) 2013

Examples of failure to detect errors

TABLE IV. Observed passing rates using the TG-119 instructions, i.e., 3%G/3 mm, 10% dose threshold, and (when available) measurement uncertainty turned “on.”

ID	Observed passing rates (%)	Details
1	99.2 ± 0.7 (1SD, range 98.1–99.8)	Mean over 7 IMRT beams
2	99.4 ± 1.2 (96.7–100)	Mean over 7 IMRT beams
3	99.3 ± 0.6 (98.9–100)	Mean over 5 IMRT beams
4A	96.6	Composite plan dose, 5 IMRT beams
4B	95.9	Composite plan dose, 1 VMAT beam
5	93.9 ^a , 94.7 ^b	Composite plan dose, 2 VMAT beams
6	97.8	Composite plan dose, 1 open field
7	100	Composite plan dose, 2 VMAT beams

^aAC.

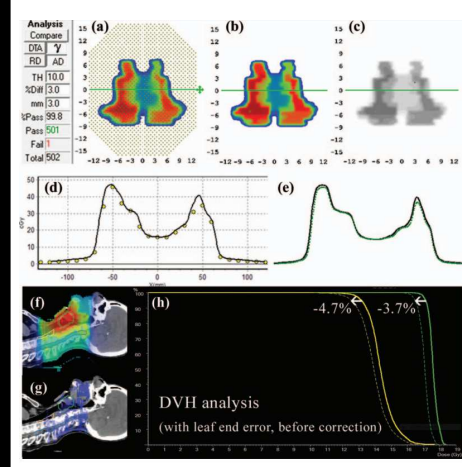
^bDelta4.

Nelms et al. Med Phys 40 (11) 2013

Examples of failure to detect errors

Case Study 1: Incorrect TPS settings

- This case presented a 99.2% MapCHECK 3%/3 mm passing rate (*averaged over all beams*) for a head and neck3
- It was noticed that the measured dose profiles were consistently slightly “inside” the calculated profiles
- A geometric scaling error during QA measurement was initially suspected
- Eventually, it was found that the leaf-end modeling was not set correctly, causing the TPS to calculate each segment slightly too wide (on the order of 1 mm)
- This had an additive effect that was quite large over many segments

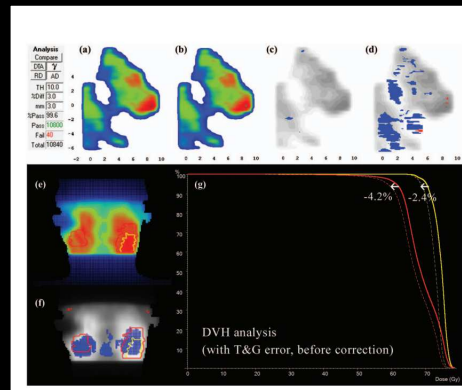


Nelms et al. Med Phys 40 (11) 2013

Examples of failure to detect errors

Case Study 2: Incorrect TPS settings

- This case presented a 3%/3 mm passing rates were high (99.4% *average over all beams*)
- More sensitive 2%/2 mm analysis showed a cold (blue) horizontal striping pattern in dose difference, an indicator of tongue-and-groove effect not being accounted for in the TPS model
- After turning “on” the T and G correction in the TPS by improving the fluence resolution to 1 mm, the meas < calc dose differences dissipated per beam 2%/2 mm analysis

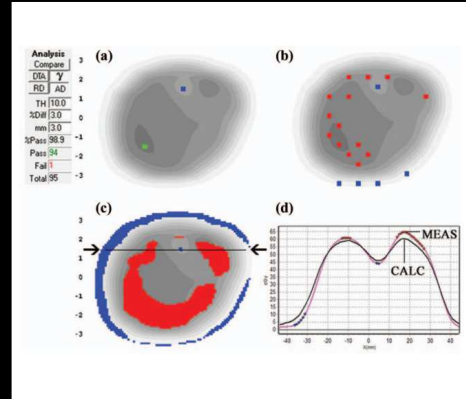


Nelms et al. Med Phys 40 (11) 2013

Examples of failure to detect errors

Case Study 3: Incorrect TPS settings

- This case presented a 3%/3 mm passing rates were high (99.3% average over all beams)
- Inspection of dose profiles and 2%/2 mm analysis showed clear, systematic dose gradient errors with the TPS underestimating dose in “peaks” and overestimating dose in “valleys”
- Measurements were repeated with a higher resolution EPID-based dosimeter (EPIDose), which yielded consistent error patterns
- The error here was due to the fact that the dose profiles used for beam modeling were acquired with a Farmer chamber and were thus blurred due to volume-averaging

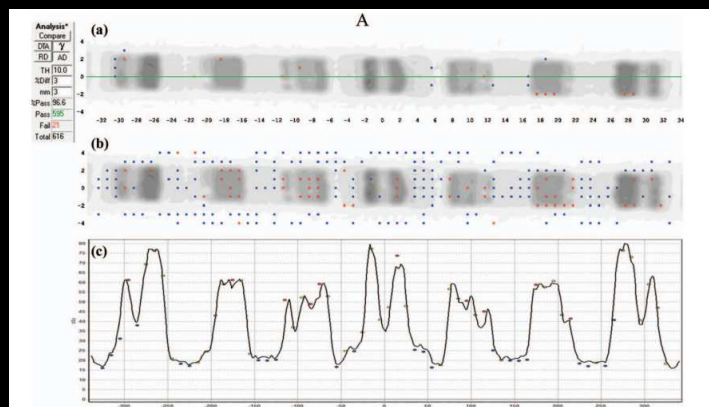


Nelms et al. Med Phys 40 (11) 2013

Examples of failure to detect errors

Case Study 4A: Incorrect TPS settings

- A 7-beam IMRT plan was analyzed via composite dose to a cylindrical phantom with a 3%/3 mm passing rate of 96.6%

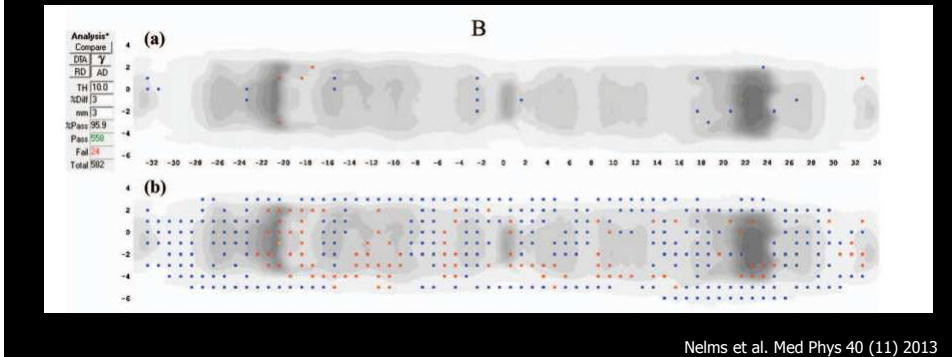


Nelms et al. Med Phys 40 (11) 2013

Examples of failure to detect errors

Case Study 4B: Incorrect TPS settings

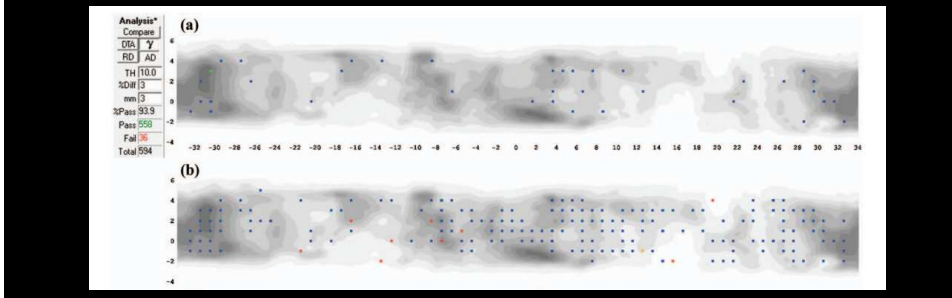
- VMAT plan for the same patient was analyzed with a 3%/3 mm passing rate of 95.9%
- In this case, the TPS employed vendor-supplied dose models that were not adjustable by the end user
- Therefore, the issue is assumed to be a TPS algorithm limitation



Examples of failure to detect errors

Case Study 5: Incorrect TPS settings

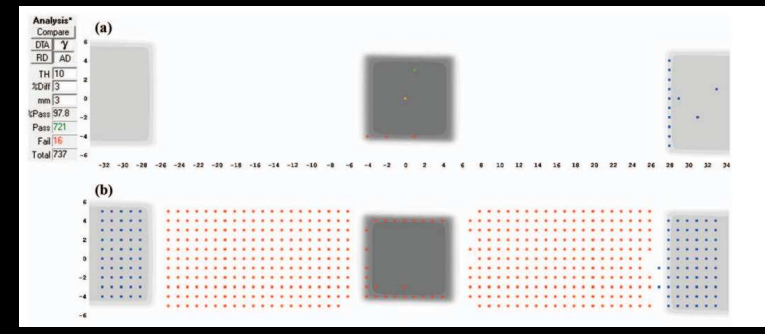
- Two arc VMAT plan with a 3%/3 mm passing rate of 94.7%
- It was found that the vast majority of VMAT segments in both arcs were very narrow, often on the order of a few mm in width
- The TPS model systematically overestimates the dose for such narrow segments
- Normally, such segments make up a relatively small portion of the field and the error is negligible



Examples of failure to detect errors

Case Study 6: Incorrect Phantom Density

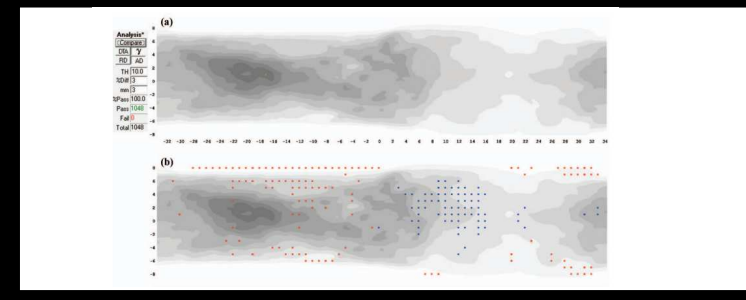
- In this case, a simple $10 \times 10 \text{ cm}^2$ field on the ArcCHECK phantom gave a high 3%/3 mm passing rate of 97.8% even with the wrong phantom density in the TPS
- The source of the error was an erroneous assignment in the TPS of an electron density of 1.11 relative to water for the uniform PMMA phantom, which should have been set equal to 1.147



Examples of failure to detect errors

Case Study 6: Incorrect Phantom Alignment

- In this case, a two arc VMAT plan had a 3%/3 mm passing rate of 100%
- The physical phantom setup on the couch was carefully verified, thus suggesting the source of the error might be an alignment error in the virtual QA phantom
- By inspecting the extents of the calculated dose grid, it was found that the plan isocenter in fact did not coincide with the center of the virtual phantom; rather, it was shifted 2.75 mm in the lateral direction



Questions